NASA TECHNICAL MEMORANDUM

NASA TM X-1734

NASA TM X-1734

THERMAL AND DIELECTRIC PROPERTIES OF A HOMOGENEOUS MOON BASED ON MICROWAVE AND INFRARED TEMPERATURE OBSERVATIONS

by Ted A. Calvert

George C. Marshall Space Flight Center
Huntsville, Ala.

NATIONAL AERONAUTICS AND SPACE ADMINISTRATION • WASHINGTON, D. C. • FEBRUARY 1969

NASA TM X-1734

THERMAL AND DIELECTRIC PROPERTIES OF A HOMOGENEOUS MOON BASED ON MICROWAVE AND INFRARED TEMPERATURE OBSERVATIONS

By Ted A. Calvert

George C. Marshall Space Flight Center
Huntsville, Ala.

NATIONAL AERONAUTICS AND SPACE ADMINISTRATION

For sale by the Clearinghouse for Federal Scientific and Technical Information
Springfield, Virginia 22151 – CFSTI price $3.00

TABLE OF CONTENTS

LIST OF ILLUSTRATIONS

LIST OF ILLUSTRATIONS (Concluded)

LIST OF TABLES

THERMAL AND DIELECTRIC PROPERTIES OF A HOMOGENEOUS MOON BASED ON MICROWAVE AND INFRARED TEMPERATURE OBSERVATIONS

SUMMARY

A homogeneous lunar model was used to establish theoretically the relationship of the thermal properties of the moon to its dielectric properties. This was accomplished using lunar observational data obtained in the microwave and infrared wavelengths. Measured values of loss tangent, dielectric constant, and thermal diffusivity for postulated lunar materials are compared to values calculated from microwave and infrared observations. Lunar microwave brightness temperatures are compared to subsurface temperatures based on selection of a thermal parameter and a depth into the lunar interior.

The measured values of loss tangent and dielectric constant for the postulated materials agree with the values based on lunar observations; however, it is not possible to establish which sample offers the best comparison. The microwave brightness temperature curves do not offer good agreement with the calculated subsurface temperatures since the phase lag and amplitudes could not be made to agree simultaneously. As a result, it may be possible to use the homogeneous model to relate the electrical properties of the lunar material to its thermal properties.

INTRODUCTION

This report relates the dielectric and thermal properties of a homogeneous moon based on calculations using microwave and infrared observational data of the moon. The calculations are compared to measured dielectric and thermal properties of materials thought to be similar to that of the moon to determine if the homogeneous model is sufficient for making calculations concerning the moon.

The experimental data used in these calculations are published data of experimentalists working in areas of microwave and infrared astronomy, and thermal and dielectric properties of materials.

LUNAR MODEL AND FOURIER HEAT EQUATION

General Parameters

The moon is assumed to be a smooth homogeneous solid which conducts heat in the manner of an isotropic body. Mathematically, the moon is considered to be a semi-infinite solid. The surface temperature is a harmonic function of time and the period of rotation is full moon to full moon (2.55×10^6 seconds).

The model is of density ρ (g/cm^3), thermal conductivity K (W/cm °K), and heat capacity C(J/g °K) and is of dielectric material with negligible magnetic loss. The magnetic permeability is considered to be that of free space.

Fourier Heat Equation

The thermal behavior of the lunar model is represented by the Fourier conduction equation for one dimension in an isotropic body; hence,

$$\frac{\partial^2 T}{\partial x^2} - \frac{1}{\alpha} \frac{\partial T}{\partial t} = 0 \qquad (x \geq 0, t > 0). \tag{1}$$

The boundary conditions to be applied are

(a) T is finite as $x \rightarrow \infty$;

(b) $T(x,t)\big|_{x=0} = T(0,t) = f(t)$

where $f(t) = A_0 + \sum_{n=1}^{\infty} A_n \cos\left(\frac{2n\pi t}{P}\right) + B_n \sin\left(\frac{2n\pi t}{P}\right)$.

Using the solution of Ingersoll [1], assuming the solution to be periodic, and applying boundary condition (a), the solutions to the differential equation are as follows:

$$T_1 = A_1 e^{-x\sqrt{\omega/2\alpha}} \left[\cos\left(\omega t - x\sqrt{\omega/2\alpha}\right)\right] \tag{2}$$

$$T_2 = A_2 e^{-x\sqrt{\omega/2\alpha}} \left[\sin\left(\omega t - x\sqrt{\omega/2\alpha}\right)\right] . \tag{3}$$

By adding the two solutions, using the principal of superposition to account for boundary condition (b), the solution becomes

$$T = A_0 + \sum_{n=1}^{\infty} e^{-x\sqrt{n\pi/\alpha P}} \left[A_n \cos\left(\frac{2n\pi t}{P} - x\sqrt{n\pi/\alpha P}\right) + B_n \sin\left(\frac{2n\pi t}{P} - x\sqrt{n\pi/\alpha P}\right)\right]. \tag{4}$$

The temperature is exponentially damped by $e^{-x\sqrt{n\pi/\alpha P}}$ as x is increased, indicating lower temperatures beneath the surface. Also, the time at which a temperature wave at depth $x \neq 0$ reaches a maximum and the time at which the surface temperature reaches a maximum will be different. This lag in time is given by

$$t = \frac{x}{2}\sqrt{\frac{P}{\pi\alpha}} \tag{5}$$

FOURIER SERIES APPROXIMATION TO LUNAR INFRARED SURFACE TEMPERATURES

Measurements of lunar surface infrared temperatures may be represented by

$$T = A_0 + \sum_{n=1}^{\infty} A_n \cos\left(\frac{2n\pi t}{P}\right) + B_n \sin\left(\frac{2n\pi t}{P}\right), \tag{6}$$

where A_0, A_n, and B_n are computed for the number of terms necessary to represent the measured values of temperature to the accuracy desired. Calculations of these coefficients are accomplished for discrete data using the following relations [2]:

$$A_0 = 1/2N \sum_{r=-N+1}^{N} f(t_r) \quad , \tag{7}$$

$$A_K = 1/N \sum_{r=-N+1}^{N} f(t_r) \cos K t_r, \ (K \neq 0, N), \tag{8}$$

$$A_N = 1/2N \sum_{r=-N+1}^{N} f(t_r) \cos N t_r \quad , \tag{9}$$

$$B_K = 1/N \sum_{r=-N+1}^{N} f(t_r) \sin K t_r \quad . \tag{10}$$

This representation of the surface data allows calculations of temperatures below the surface at any depth x. An example of the approximation to the surface data and calculations of subsurface temperatures is shown in Figure 1.

GENERAL MICROWAVE THEORY

Observation and analysis of the behavior of the electromagnetic radiation emitted from the moon enables one to determine the physical characteristics of the lunar material. Figure 2 [3] illustrates radiation from a point beneath the surface of the moon. As the radiation moves from point p toward the surface, it is subject to both absorption and re-emission by the lunar material. Further, the radiation is subjected to the reflective and refractive properties of the lunar material. Details of these phenomena are omitted from this text and the reader is referred to Weaver [3].

The intensity of radiation emitted from beneath the surface is converted to temperature for radio telescopes and the brightness temperature of the moon at any point [3] is represented by

$$T_b(\nu,\theta,t) = \left\{1 - \left(\frac{R_p(\theta) + R_s(\theta)}{2}\right)\right\} \left\{T_0 + \frac{T_1}{a_1(\theta)} \cos[\Omega t - \xi_1] + \frac{T_2}{a_2(\theta)} \cos[2\Omega t - \xi_2] + \ldots\right. \quad (11)$$

T_0 is the constant component of the surface temperature; T_1 and T_2 are amplitudes of the first and second harmonic temperature. Additionally, $a_1(\theta)$ and $a_2(\theta)$ are the amplitude attenuation factors with ξ_1, and ξ_2 the phase lag of the harmonics.

The problem is simplified by restricting the temperature variation to the center of the lunar disc in which case $\theta = 0$. Thus, the effective brightness temperature becomes [4]:

$$T_E = (1 - R_\perp)\left[A_0 + \frac{A_1}{a_1(0)} \cos(\Omega t - \xi_1] + \frac{A_2}{a_2(0)} \cos(2\Omega t - \xi_2) + \ldots,\right] \quad (12)$$

where the reflection coefficient is [4]

$$R = \left[\frac{\sqrt{\epsilon} - 1}{\sqrt{\epsilon} + 1}\right]^2 \quad (13)$$

and ϵ is the relative dielectric constant of the lunar material.

THERMAL AND DIELECTRIC RELATIONSHIPS

Using the solution to the Fourier heat conduction equation and the modified equation for the intensity of radiation emitted from the moon, it is possible to formulate a relationship between the thermal diffusivity and the dielectric conductivity of a material and compute its dielectric constant and loss tangent. The thermal wave, as shown previously, is damped by a factor $e^{-x\sqrt{n\pi/\alpha P}}$. At some depth, x, the damping term will become e^{-1}. The depth x is termed the depth of penetration, denoted l_t, of the thermal wave and is given by the following expression:

$$l_t = (\alpha P/\pi)^{\frac{1}{2}}. \tag{14}$$

Also, there is a relationship between the depth of penetration of the thermal wave and the depth of penetration of the electromagnetic wave; i.e.,

$$l_e = \delta l_t , \tag{15}$$

where l_e is the depth of penetration of the electromagnetic wave and δ is the solution to the equation [5]

$$(1 + 2\delta + 2\delta^2)^{\frac{1}{2}} = \frac{\bar{T}e_0}{\bar{T}e_1} \frac{B_1}{B_0} \frac{T_1(0)}{T_0(0)} . \tag{16}$$

with $\bar{T}e_0$ and $\bar{T}e_1$ being the first and second terms in a Fourier Series approximation to the microwave temperature throughout a lunation; B_1 and B_0 are averaging coefficients assumed to be unity; $T_0(0)$ and $T_1(0)$ are the first and second terms in a Fourier series approximation to the infrared surface temperatures throughout a lunation. The reflection coefficient for perpendicular incidence of radiation on the moon is given by

$$R_\perp = 1 - \frac{\bar{T}e_0}{B_0\, T_0(0)} . \tag{17}$$

If the reflection coefficient for perpendicular incidence is known the dielectric constant may be calculated by the relation

$$\epsilon = \left[\frac{-(R^{\frac{1}{2}}+1)}{(R^{\frac{1}{2}}-1)}\right]^2 \quad . \tag{18}$$

The depth of penetration of the electromagnetic wave (attenuation distance) [6] is also given by

$$l_e = \frac{\lambda}{4\pi\,\epsilon^{\frac{1}{2}}} \left\{-\tfrac{1}{2} + \tfrac{1}{2}\left[1 + (\tan\Delta)^2\right]^{\frac{1}{2}}\right\}^{-\frac{1}{2}} . \tag{19}$$

The solution of this equation for tan Δ gives the loss tangent as

$$\tan\Delta = \left\{\left[(\lambda^2/8\pi^2\,\epsilon\, l_e^{\,2}) + 1\right]^2 - 1\right\}^{\frac{1}{2}} \quad . \tag{20}$$

In terms of the thermal diffusivity equation (20) becomes

$$\tan\Delta = \left\{\left[(\lambda^2/8\pi\,\epsilon\,\alpha\,\delta^2 P) + 1\right]^2 - 1\right\}^{\frac{1}{2}} \quad . \tag{21}$$

Thus, a relationship between the loss tangent and the thermal diffusivity is established and may be simplified to read

$$\tan\Delta = (c_1^{\,2}\,\alpha^{-2} + 2c_1\alpha^{-1})^{\frac{1}{2}} \quad , \tag{22}$$

where $c_1 = \lambda^2/8\pi\epsilon\delta^2 P$.

The dielectric conductivity is given by the expression

$$\sigma = 2\pi \tan\Delta\, \nu\, \epsilon\, \epsilon_0 \quad , \tag{23}$$

where ν is the frequency of the radiation and ϵ_0 is the dielectric constant of free space.

Substitution for tan Δ gives the dielectric conductivity as a function of thermal diffusivity, thus

$$\sigma = K_1\alpha^{-2} + K_2\alpha^{-1} \quad , \tag{24}$$

with $K_1 = \frac{\nu^2\epsilon_0^2\lambda^4}{16\,\delta^4 P^2}$ and $K_2 = \frac{\pi\nu^2\,\epsilon\,\epsilon_0^2\,\lambda^2}{\delta^2 P}$.

Hence, relationships are established which relate the thermal properties of a simulated lunar material to the dielectric properties. These relationships are given parametrically in Figures 3 and 4.

The calculations for Figures 3 and 4 are based on infrared data Set I and Set II, respectively. Under the conditions of this model, it is possible to compare the behavior of the dielectric conductivity with that of thermal diffusivity. For example, consider the laboratory-measured value of basalt powder at 3.28 cm to be 1.681×10^{-5} cm^2/ sec. The dielectric conductivity then ranges from 1.2×10^{-4} to 2.0×10^{-4} MΩ /m when considering the microwave measurements in the wavelength range 3.15 to 3.20 cm.

It is also interesting to note that for fixed thermal diffusivity there is a pronounced shifting of the parameter lines toward larger values of dielectric conductivity as the wavelength of microwave observation decreases. Also, comparison of Figure 3 with Figure 4 denotes a slight shift toward larger values of dielectric conductivity for fixed thermal diffusivity. This shows that differences in surface temperatures do cause different results although apparently not so drastic as the changing of wavelength of microwave observations.

To refine this portion of the analysis requires that selected laboratory samples be chosen and their thermal and dielectric properties be observed at predetermined wavelengths. Simultaneously, microwave observations should be obtained at the same wavelength. Additionally, the refinement of the surface temperatures throughout a lunation should be continued, especially at or near midnight and pre-dawn.

EXPERIMENTAL DATA

The experimental data used in comparisons and calculations related in this study are from published reports in areas of infrared and microwave astronomy and measurements of postulated lunar materials.

The infrared measurements used were published by Low [7], Sinton [8], Saari [9], and Murray and Wildey [10]. These data are shown in Figures 5 and 6. For this study, the infrared data were combined into two sets of data. Infrared data Set I consisted of the data published by Sinton, Low, and Saari. Infrared data Set II consisted of data published by Sinton, Low, and Murray and Wildey. A curve representing the surface temperatures was drawn through the data points and temperature values read at even intervals throughout the period. These values were then used in the Fourier series approximation to the lunar surface temperatures. Figure 7 shows the surface curve as represented by the Fourier series approximation to the combined data of Saari, Sinton, and Low. Also shown are the surface data with a difference curve between the data and the approximation.

The microwave measurements used are shown in Table I [4]. These measurements were chosen primarily because the wavelengths at which the observations were made are comparable to the wavelength at which the measurements of the simulated lunar materials were made.

The A. D. Little Laboratory measurements of dielectric constant [11], loss tangent, and thermal diffusivity were used in order to make comparisons of calculated values with measured values of these quantities. The calculated values of dielectric constant and loss tangent were obtained using the diffusivity values for basalt (as measured by A. D. Little) and the microwave measurements listed in Table I. Table II shows the measured data which were compared to the calculated values.

TEST OF THE HOMOGENEOUS MODEL

The adequacy of the homogeneous model is tested according to the method presented by Weaver [3]. The phase lag of the first harmonic, was plotted as a function of the observed amplitude attenuation factor a_1, where a_1 is given by

$$1 + 2\,\delta + 2\delta^2 = a_1^2 \quad . \tag{25}$$

The calculated values should fall on the theoretical curve of Figure 8 so that the homogeneous model accurately represents the observations. The model is considered inaccurate if the values of a_1 are consistently above the theoretical curve. Weaver does not consider this to be a discriminating test because of the manner in which the ratios $A_0/(A_1/a_1)$ are established.

The values of phase lag are taken from the observational data. The factor δ is calculated based on the observational data using equation (16), and a_1 is then calculated using equation (25). These values are then plotted on the theoretical curve denoting the relationship of these factors. Figure 8 shows how the observational data compare to the theoretical values. This comparison denotes that the homogeneous model does fit the observational data in a representative manner.

RESULTS

Calculations of dielectric conductivity as a function of thermal diffusivity are shown in Figures 3 and 4. Figure 3 is based on the microwave data of the authors indicated on the figure, and the infrared data are shown in Figure 5. Figure 4 is based on the same microwave data and the infrared data of Figure 6. As a result of the calculations of dielectric conductivity, the equation $\sigma = K_1\alpha^{-2} + K_2\alpha^{-1}$ was reduced to $\sigma = \sqrt{K_2\alpha}^{-\frac{1}{2}}$, allowing a simplified relationship between dielectric conductivity and thermal diffusivity. Table III gives the values of $\sqrt{K_2}$ for the microwave data considered.

Table II compares the calculated values of dielectric constant and loss tangent of the homogeneous model to laboratory measurements of postulated lunar materials. The powders offer better comparison than the solid materials, but it cannot be said which of the two powders compares best for values of dielectric constant. Figures 9 and 10 offer a graphical comparison of loss tangent values with basalt making the better comparison. The data of Mayer, McCullough, and Slonaker offer the best comparison to the loss tangent values of basalt and pumice powders, but it is difficult to say which observational data best compares the calculated and measured values of dielectric constant. Figures 11, 12, and 13 compare the calculated and measured values of dielectric constant. The test of the homogeneous model indicates that the calculations of the amplitude attenuation factor from observational data are in general agreement with the theoretical curve, although some values do not appear acceptable.

The calculations of temperature and phase lag at depths below the lunar surface are compared to microwave observations in Figures 14 and 15.* Each set of microwave observational data shown in Table III was used in turn to generate a brightness temperature curve throughout a lunation. Since the constant component, phase lag, and the first harmonic differ between observers,

*In Figure 14, the calculated subsurface curve is based on infrared data Set I and is the same in all parts of Figure 14. Likewise, in Figure 15, the calculated subsurface curve is based on infrared Set II and is the same in all of Figure 15.

the generated brightness temperature curves differ accordingly. These brightness temperature curves were compared to the subsurface temperature curves calculated, based upon the infrared data of Set I and Set II, respectively.

It was anticipated that these comparisons would allow a subsurface temperature curve to correspond to a brightness temperature. The brightness temperature curves are indicated by the observer's name and the wavelength at which the observations were made. The calculated subsurface temperatures are indicated by type of material and the depth of penetration of the thermal wave.

These comparisons are not acceptable, in general, since the microwave temperature values do not properly coincide with the infrared subsurface temperatures at a depth. The depth was selected based on solution of equation (14). It should be noted that the depth of penetration of the thermal wave differs for basalt and pumice caused by different values of thermal diffusivity; however, the subsurface temperature curve is the same for both. This is because the attenuation factor, $e^{-x\sqrt{n\pi/\alpha P}}$, is set equal to e^{-1}.

Another unacceptable result of this comparison is that the time of maximum temperatures for the microwave and calculated subsurface curve do not coincide, or, simply, the values of phase lags do not agree.

These results are difficult to explain since the attenuation may extend farther than one optical depth. The fact that the microwave temperature is an integrated value over depth, and the calculated surface temperature corresponds to a particular depth, may cause this discrepancy, or it may be that the homogeneous model is inadequate.

CONCLUSION

The homogeneous model may be used to relate the electrical properties of the moon to its thermal properties. Since the surface temperatures were used in the initial boundary conditions, little can be said about its adequacy as a thermal model. The calculations of temperature and phase lag at depths below the lunar surface do not agree with the observed microwave temperature values; therefore, either the model is inadequate or the microwave data have not been treated properly so as to allow comparison with calculations made for a single point on the lunar central region.

The calculated values of dielectric constant and loss tangent agree in general with the laboratory measurements of basalt and pumice powders; however, it cannot be definitely stated which of the samples offers the better comparison. Thus, it may be impossible to determine the composition of the moon from dielectric properties using a homogeneous model.

The observational microwave data yielded different values of dielectric constant and loss tangent for different wavelengths of observations. This may be due to differences in observation techniques rather than any phenomena associating wavelength to dielectric constant.

It must be concluded that when treated in the manner of this analysis, the homogeneous model cannot be expected to generate both thermal and dielectric properties of the lunar material nor can it distinguish its composition or structure. As a result it must be considered inadequate and other models must be derived for these purposes.

George C. Marshall Space Flight Center
National Aeronautics and Space Administration
Huntsville, Alabama, June 4, 1968
908-20-03-0000-28-00-000

TABLE I. EXPERIMENTAL MICROWAVE DATA

λ[a]	T_0[b]	T_1[c]	ξ[d]	AUTHOR
0.13	216	120	16	Fedoseyev, 1963
0.40	204	56	23	Kislyakov, Plechkov, 1963
0.80	197	32	40	Salomonovich, 1958
0.80	211	40	30	Salomonovich, Losovskiy, 1962
1.63	208	37	30	Kamenskaya, Semenov, Troitskiy, Plechkov, 1962
2.00	190	20	40	Salomonovich, Koschenko, 1961
3.15	195	12	44	Mayer, McCullough, Slonaker, 1961
3.20	223	17	45	Losovskiy, Salomonovich, Koschenko, 1961
3.20	210	13.5	55	Krotikov, Porfiryev, Troitskiy, 1961
3.20	213	14	26	Bondar, Zelinskaya, Porfiryev, Strezhneva, 1962
3.20	216	16	15	Bondar, 1962

a. λ Wavelength at which observations made (cm)

b. T_0 Constant microwave temperature component (°K)

c. T_1 Amplitude of first harmonic (°K)

d. ξ Phase lag of amplitude of first harmonic (deg.)

TABLE II. CALCULATED AND MEASURED LUNAR MATERIAL PROPERTIES[a]

SAMPLE	λ	$\alpha = k/\rho c$	ϵ CALCULATED	ϵ MEASURED	LOSS TANGENT CALCULATED	LOSS TANGENT MEASURED	AUTHOR/DATE
Basalt, Powder	0.80	1.681×10^{-5}	2.67	2.8	0.0090	0.0120	Salomonovich,
Pumice, Powder	0.80	1.764×10^{-5}	2.67	1.9	0.0088	0.0070	Losovskiy, 1962
Basalt, Powder	3.15	1.681×10^{-5}	4.5	2.9	0.0078	0.0067	Mayer, McCullough,
Basalt, Solid	3.15	4.761×10^{-3}	9.9	8.6	0.00047	0.014	Slonaker, 1961
Pumice, Powder	3.15	1.764×10^{-5}	4.5	2.1	0.0076	0.0045	
Pumice, Melted	3.15	4.225×10^{-3}	14.3	5.4	0.00049	0.0072	
Basalt, Powder	3.20	1.681×10^{-5}	1.3	2.9	0.0185	0.0067	Koschenko,
Basalt, Solid	3.20	4.761×10^{-3}	1.7	8.6	0.00112	0.014	Losovskiy,
Pumice, Powder	3.20	1.764×10^{-5}	1.3	2.1	0.0180	0.0045	Salomonovich, 1961
Pumice, Melted	3.20	4.225×10^{-3}	2.0	5.4	0.00118	0.0072	
Basalt, Powder	3.20	1.681×10^{-5}	2.8	2.9	0.0105	0.0067	Krotikov,
Basalt, Solid	3.20	4.761×10^{-3}	5.5	8.6	0.00064	0.014	Porfiryev,
Pumice, Powder	3.20	1.764×10^{-5}	2.8	2.1	0.0102	0.0045	Troitskiy, 1961
Pumice, Melted	3.20	4.225×10^{-3}	7.7	5.4	0.00068	0.0072	
Basalt, Powder	3.20	1.681×10^{-5}	2.5	2.9	0.0014	0.0067	Bondar, Zelinskay[a],
Basalt, Solid	3.20	4.761×10^{-3}	4.7	8.6	0.00070	0.014	Porfiryev,
Pumice, Powder	3.20	1.764×10^{-5}	2.5	2.1	0.0110	0.0045	Strezhneva, 1962
Pumice, Melted	3.20	4.225×10^{-3}	6.6	5.4	0.00074	0.0072	
Basalt, Powder	3.20	1.681×10^{-5}	2.15	2.9	0.0140	0.0067	Bondar, 1962
Basalt, Solid	3.20	4.761×10^{-3}	3.8	8.6	0.00084	0.014	
Pumice, Powder	3.20	1.764×10^{-5}	2.15	2.1	0.0135	0.0045	
Pumice, Melted	3.20	4.225×10^{-3}	5.2	5.4	0.00089	0.0072	

a. A. D. Little Laboratory measurements were made at wavelengths 1.18 and 3.28 cm. The λ indicates the wavelength at which microwave observations were made (calculations based on infrared data Set I).

TABLE II. CALCULATED AND MEASURED LUNAR MATERIAL PROPERTIES (Concluded)

SAMPLE	λ	$\alpha = k/\rho c$	ϵ CALCULATED	ϵ MEASURED	LOSS TANGENT CALCULATED	LOSS TANGENT MEASURED	AUTHOR/DATE
Basalt, Powder	0.80	1.681×10^{-5}	2.97	2.8	0.0090	0.0120	Salomonovich,
Pumice, Powder	0.80	1.764 s 10^{-5}	2.97	1.9	0.0088	0.0070	Losovskiy, 1962
Basalt, Powder	3.15	1.681×10^{-5}	4.85	2.9	0.0078	0.0067	Mayer, McCullough,
Basalt, Solid	3.15	4.761×10^{-3}	10.79	8.6	0.00047	0.014	Slonaker, 1961
Pumice, Powder	3.15	1.764×10^{-5}	4.85	2.1	0.0076	0.0045	
Pumice, Melted	3.15	4.225×10^{-3}	15.71	5.4	0.00049	0.0072	
Basalt, Powder	3.20	1.681×10^{-5}	1.7	2.9	0.0185	0.0067	Koschenko,
Basalt, Solid	3.20	4.761×10^{-3}	2.65	8.6	0.00112	0.014	Losovskiy,
Pumice, Powder	3.20	1.764×10^{-5}	1.7	2.1	0.0180	0.0045	Salomonovich, 1961
Pumice, Melted	3.20	4.225×10^{-3}	3.48	5.4	0.00118	0.0072	
Basalt, Powder	3.20	1.681×10^{-5}	3.07	2.9	0.0105	0.0067	Krotikov,
Basalt, Solid	3.20	4.761×10^{-3}	6.16	8.6	0.00064	0.014	Porfiryev,
Pumice, Powder	3.20	1.764×10^{-5}	3.07	2.1	0.0102	0.0045	Troitskiy, 1961
Pumice, Melted	3.20	4.225×10^{-3}	8.77	5.4	0.00068	0.0072	
Basalt, Powder	3.20	1.681×10^{-5}	2.76	2.9	0.0014	0.0067	Bondar, Zelinskaya,
Basalt, Solid	3.20	4.761×10^{-3}	5.36	8.6	0.00070	0.014	Porifryev,
Pumice, Powder	3.20	1.764×10^{-5}	2.76	2.1	0.0110	0.0045	Strezhneva, 1962
Pumice, Melted	3.20	4.225×10^{-3}	7.57	5.4	0.00074	0.0072	
Basalt, Powder	3.20	1.681×10^{-5}	2.45	2.9	0.0140	0.0067	Bondar, 1962
Basalt, Solid	3.20	4.761×10^{-3}	4.56	8.6	0.00084	0.014	
Pumice, Powder	3.20	1.764×10^{-5}	2.45	2.1	0.0135	0.0045	
Pumice, Melted	3.20	4.225×10^{-3}	6.36	5.4	0.00089	0.0072	

(Calculations based on infrared data set II.)

TABLE III. VALUES OF $\sqrt{K_2}$ FOR RELATIONSHIP BETWEEN DIELECTRIC CONDUCTIVITY AND THERMAL DIFFUSIVITY,

$$\sigma = \sqrt{K_2}\,\alpha^{-\frac{1}{2}}$$

λ	$\sqrt{K_2}$	AUTHOR/DATE
0.13	0.1322×10^{-4}	Fedoseyev, 1963
0.40	0.3926×10^{-5}	Kislyakov, Plechkov, 1963
0.80	0.2198×10^{-5}	Salomonovich, 1958
0.80	0.2106×10^{-5}	Salomonovich, Losovskiy, 1962
1.63	0.2058×10^{-5}	Kamenskaya, Semenov, Troitskiy, Plechkov, 1962
2.00	0.1466×10^{-5}	Salomonovich, Koschenko, 1961
3.15	0.7626×10^{-6}	Mayer, McCullough, Slonaker, 1961
3.20	0.5164×10^{-6}	Losovskiy, Salomonovich, Koschenko, 1961
3.20	0.6268×10^{-6}	Krotikov, Porfiryev, Troitskiy, 1961
3.20	0.6044×10^{-6}	Bondar, Zelinskaya, Porfiryev, Strezhneva, 1962
3.20	0.6420×10^{-6}	Bondar, 1962

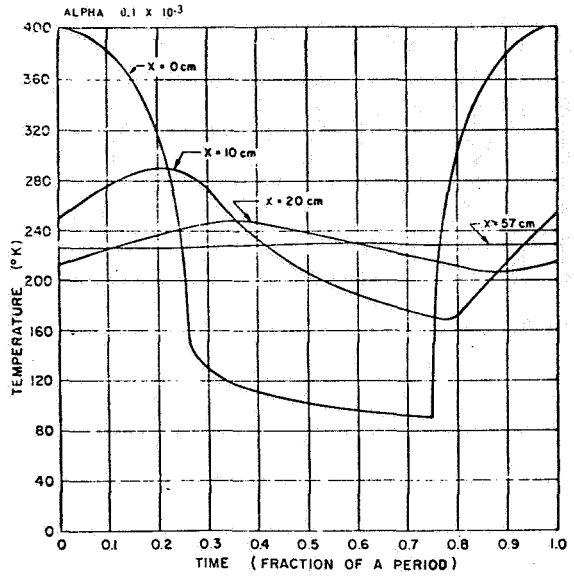

FIGURE 1. FOURIER SERIES SURFACE CURVE AND SUBSURFACE TEMPERATURES

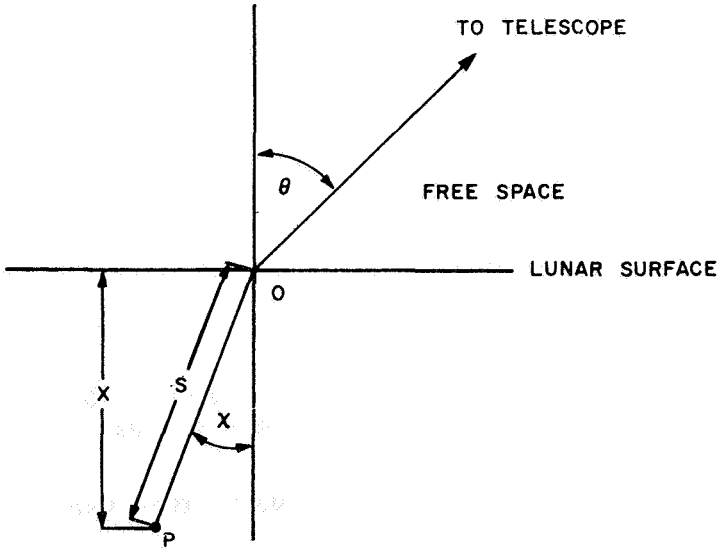

FIGURE 2. MICROWAVE EMISSION FROM THE MOON

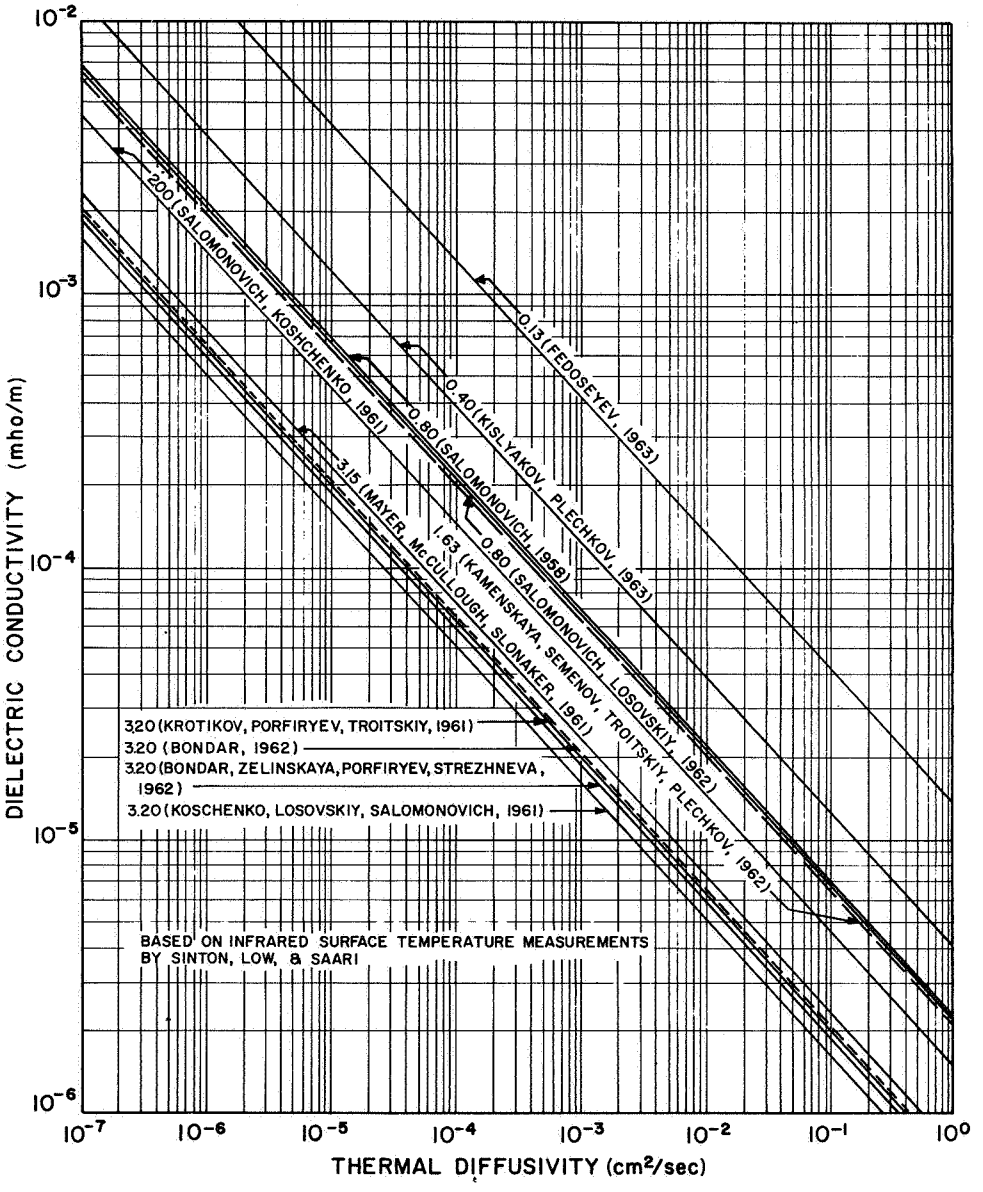

NOTE: The number preceding observer's name denotes wavelength in centimeters.

FIGURE 3. DIELECTRIC CONDUCTIVITY VERSUS THERMAL DIFFUSIVITY BASED ON INFRARED DATA SET I

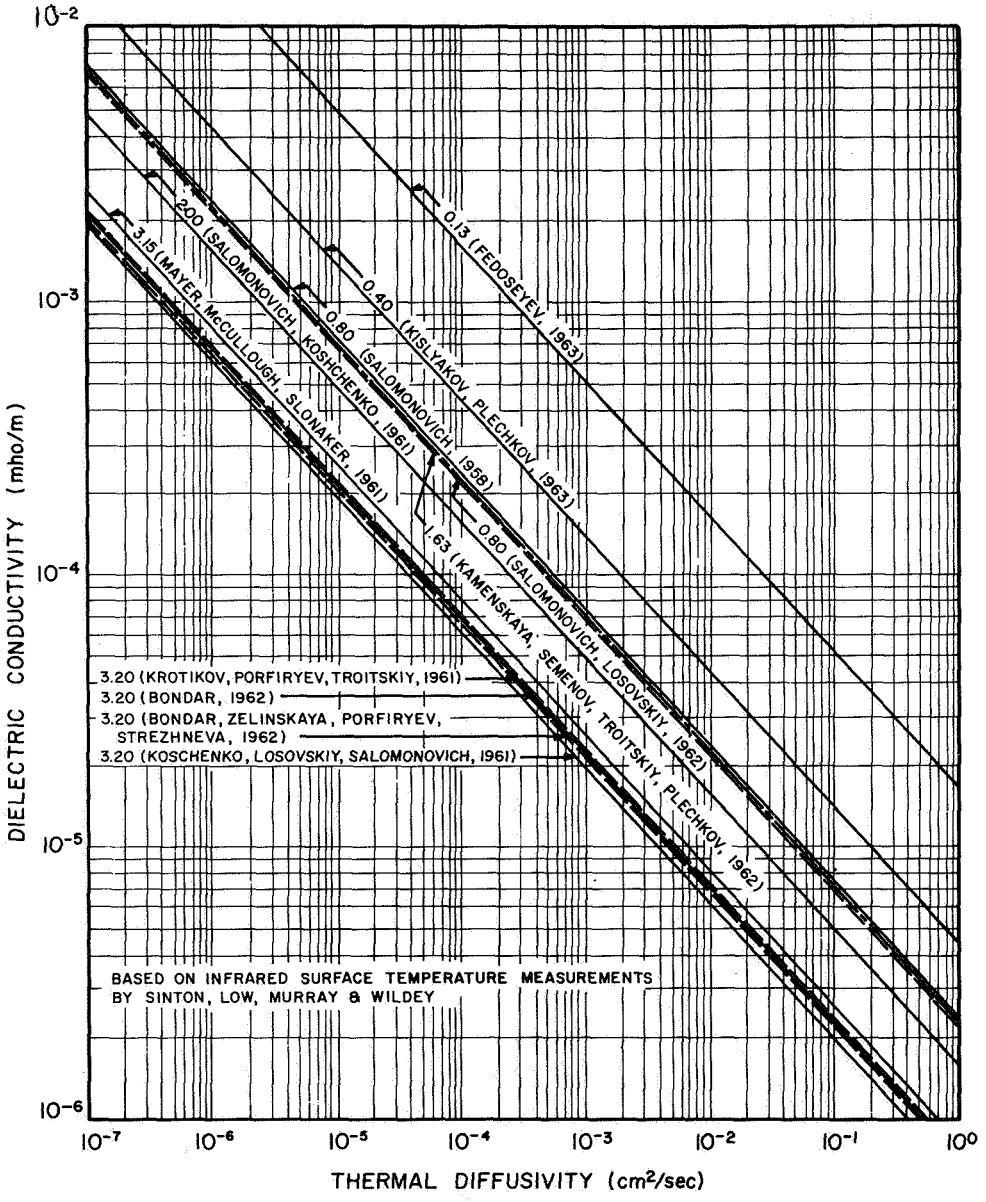

NOTE: The number preceding observer's name denotes wavelength in centimeters.

FIGURE 4. DIELECTRIC CONDUCTIVITY VERSUS THERMAL DIFFUSIVITY BASED ON INFRARED DATA SET II

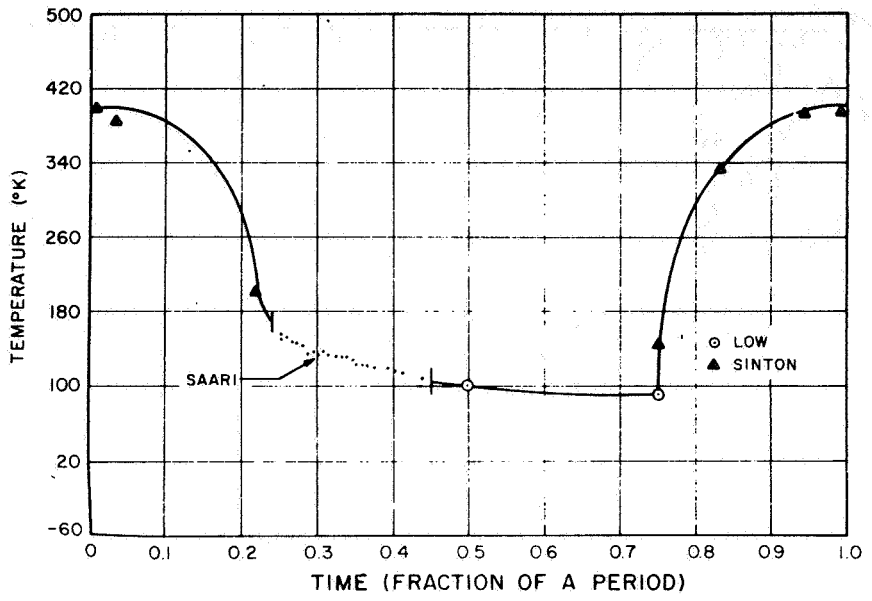

FIGURE 5. LUNAR SURFACE TEMPERATURE DATA OF LOW, SINTON, AND SAARI

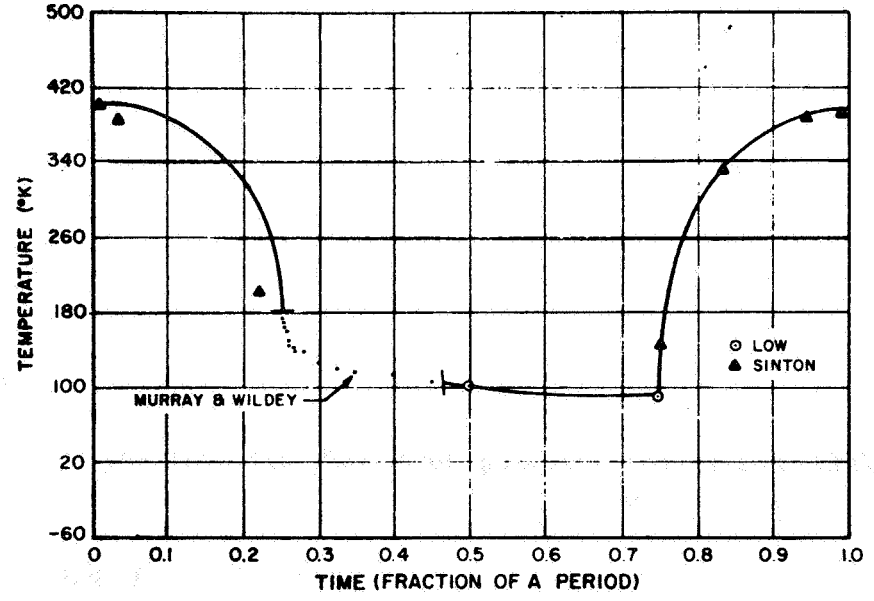

FIGURE 6. LUNAR SURFACE TEMPERATURE DATA OF LOW, SINTON, MURRAY, AND WILDEY

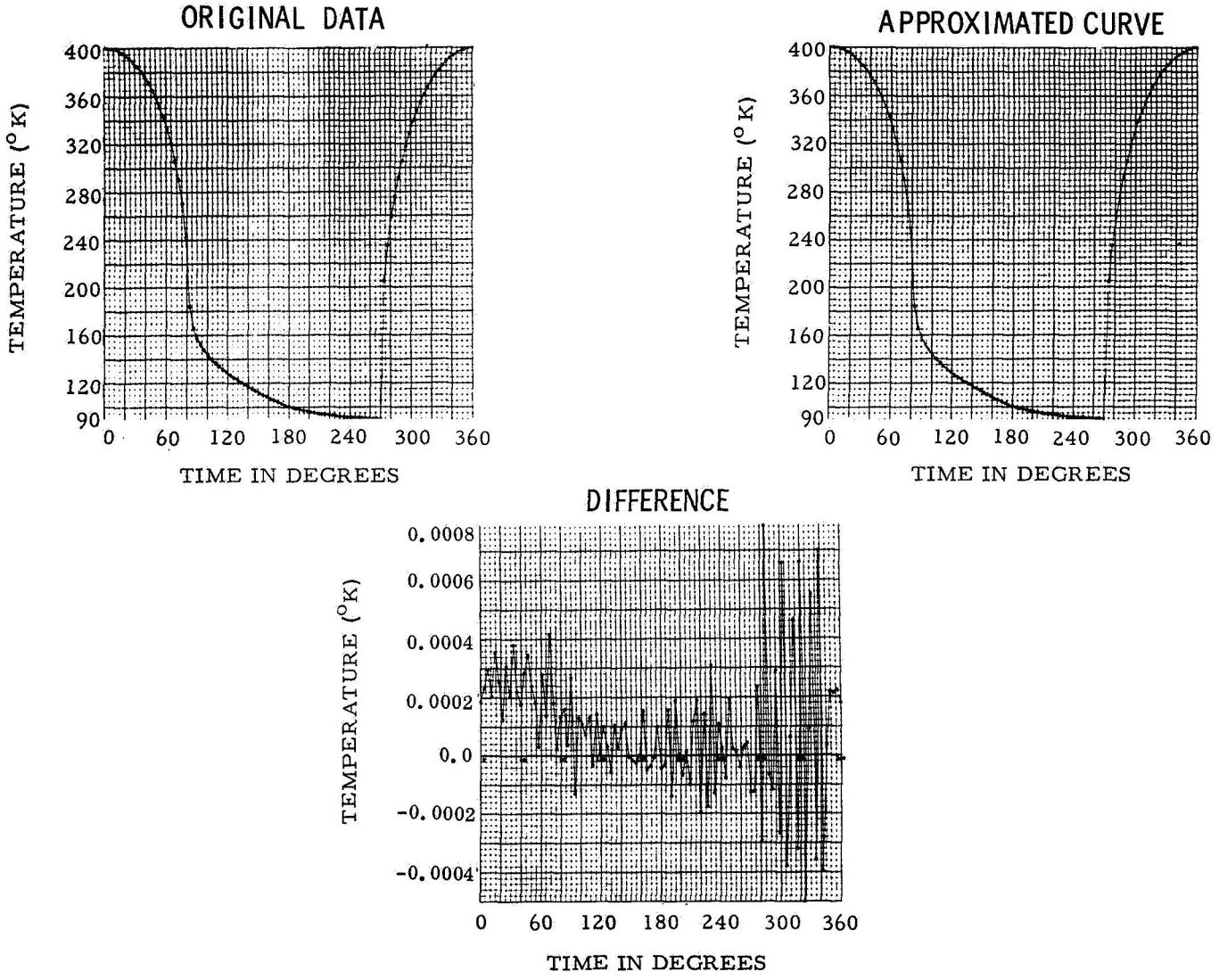

FIGURE 7. FOURIER SERIES APPROXIMATION TO SURFACE TEMPERATURES

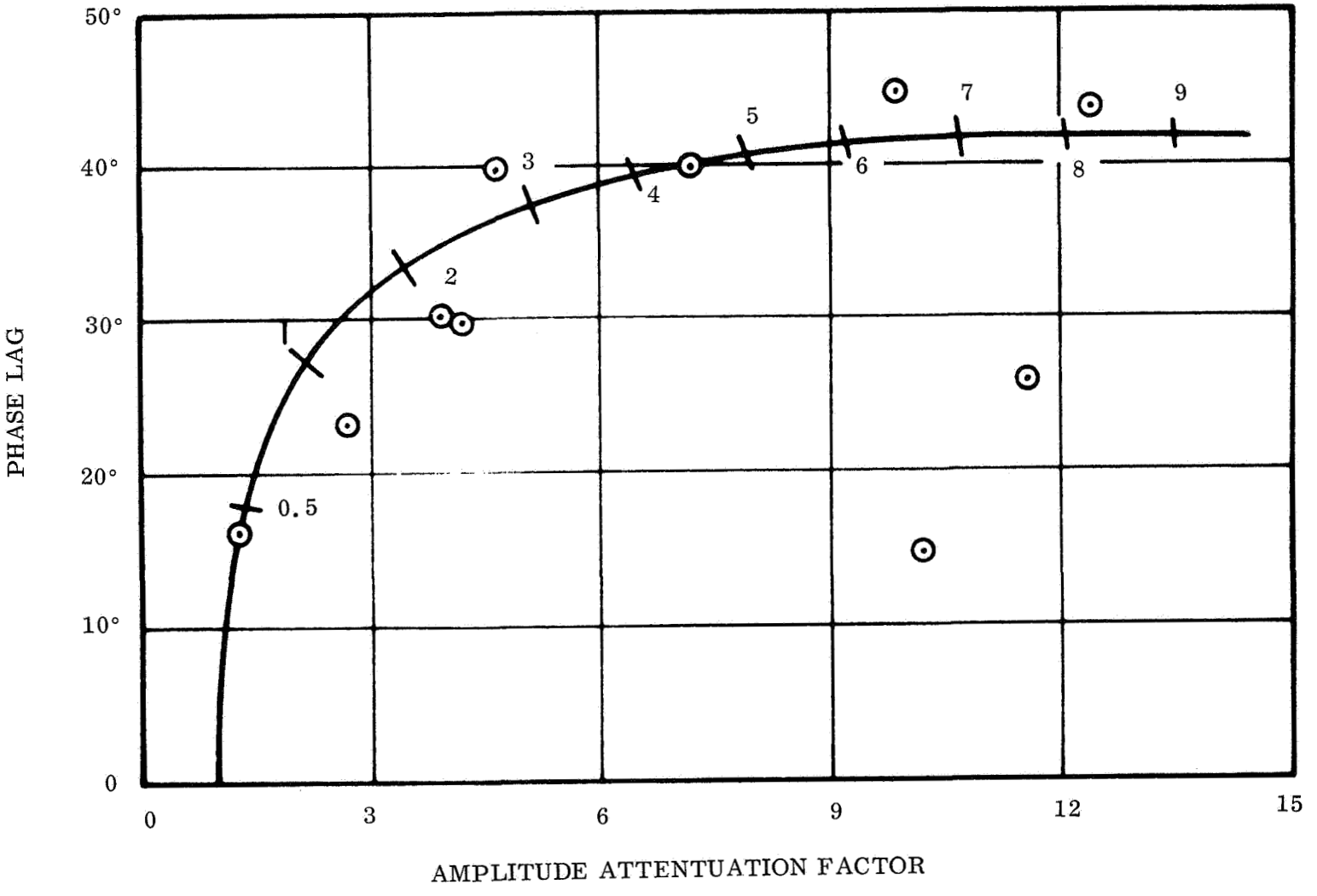

FIGURE 8. AMPLITUDE ATTENUATION FACTOR AND PHASE LAG

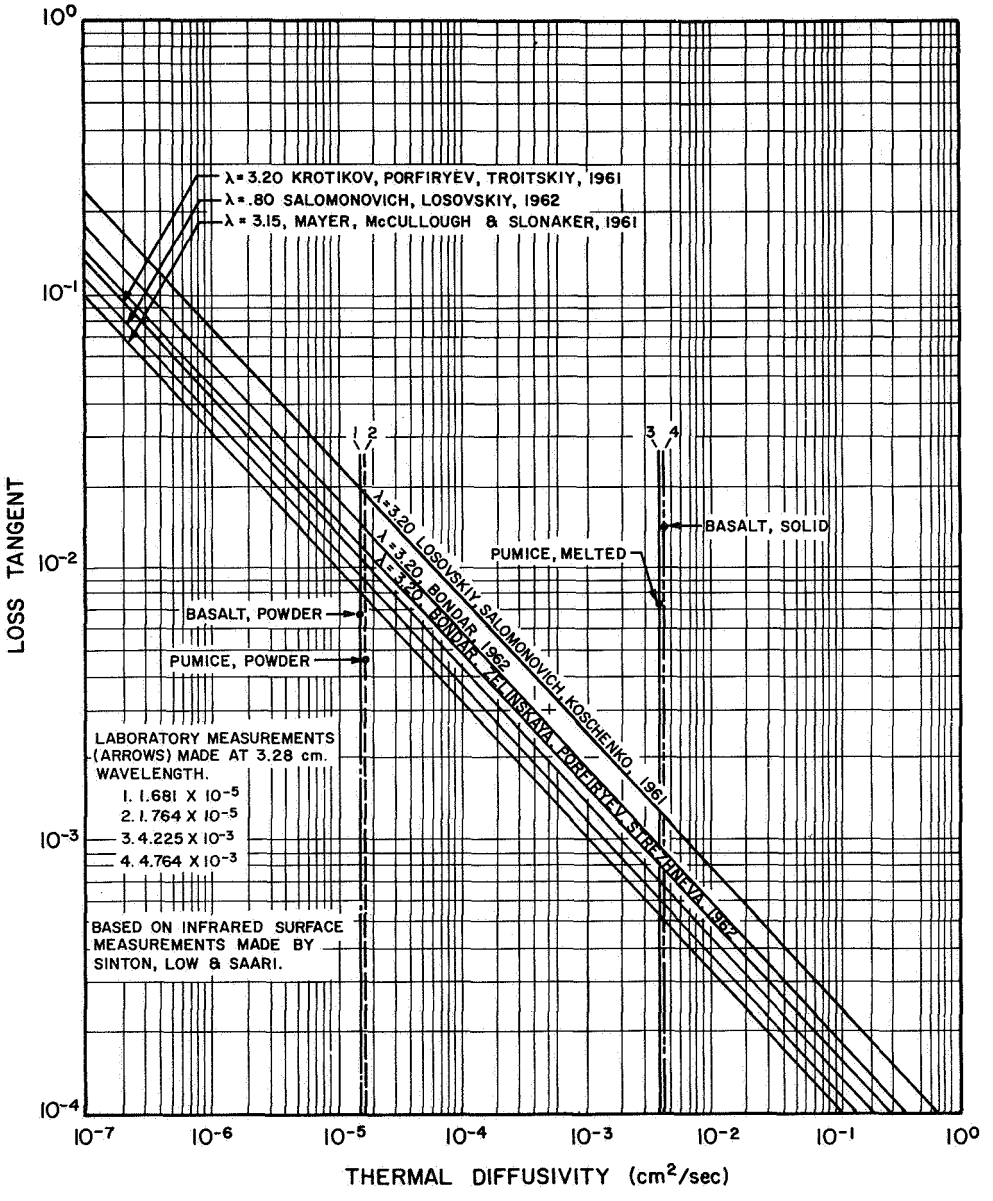

FIGURE 9. LOSS TANGENT VERSUS THERMAL DIFFUSIVITY; LABORATORY MEASUREMENTS COMPARED TO CALCULATED VALUES BASED ON INFRARED DATA, SET I

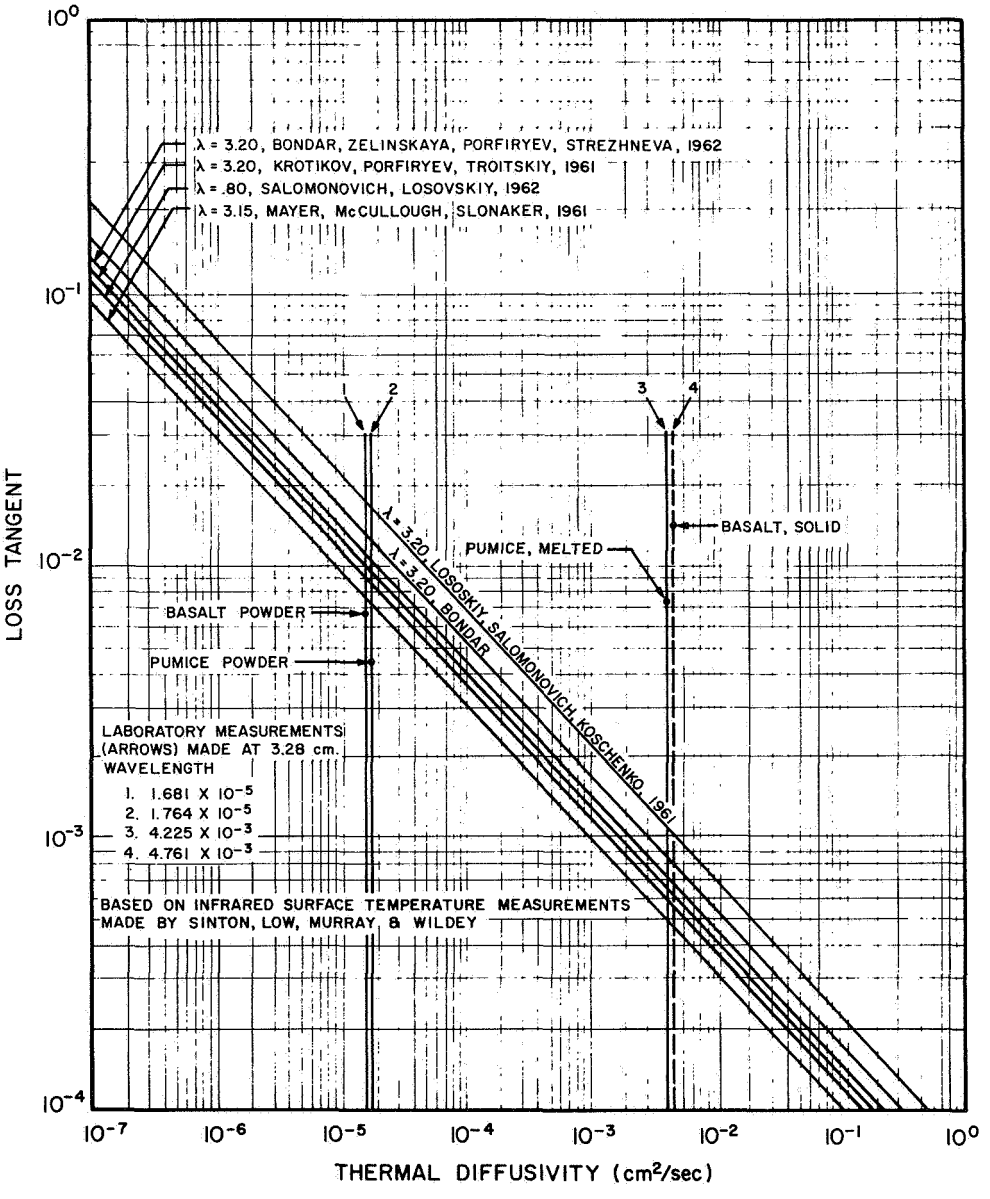

FIGURE 10. LOSS TANGENT VERSUS THERMAL DIFFUSIVITY; LABORATORY MEASUREMENTS COMPARED TO CALCULATED BASED ON INFRARED DATA, SET II

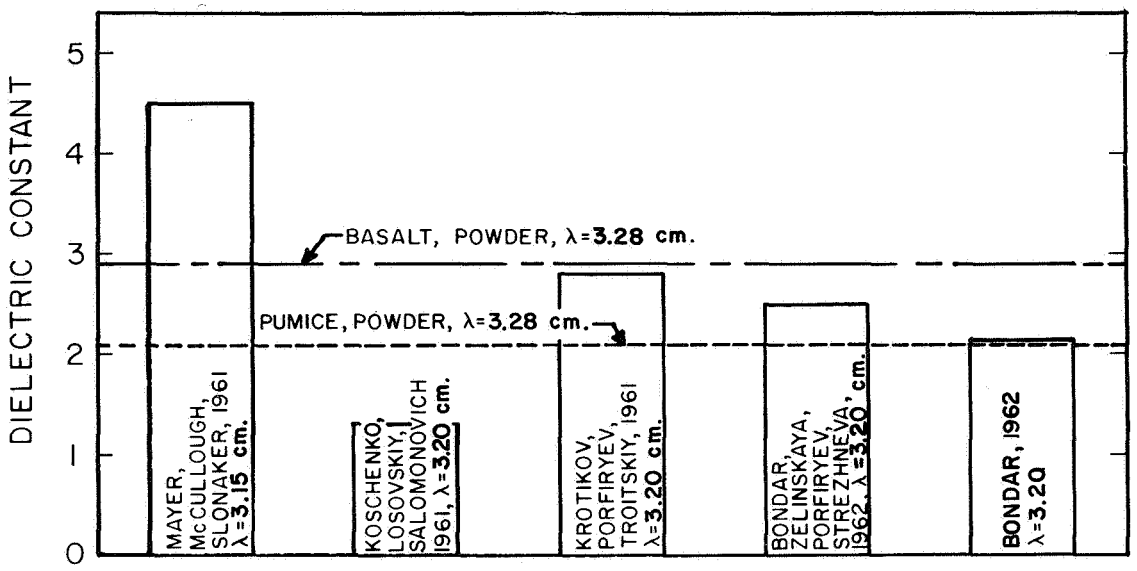

FIGURE 11. DIELECTRIC CONSTANT VALUES BASED ON INFRARED DATA, SET I

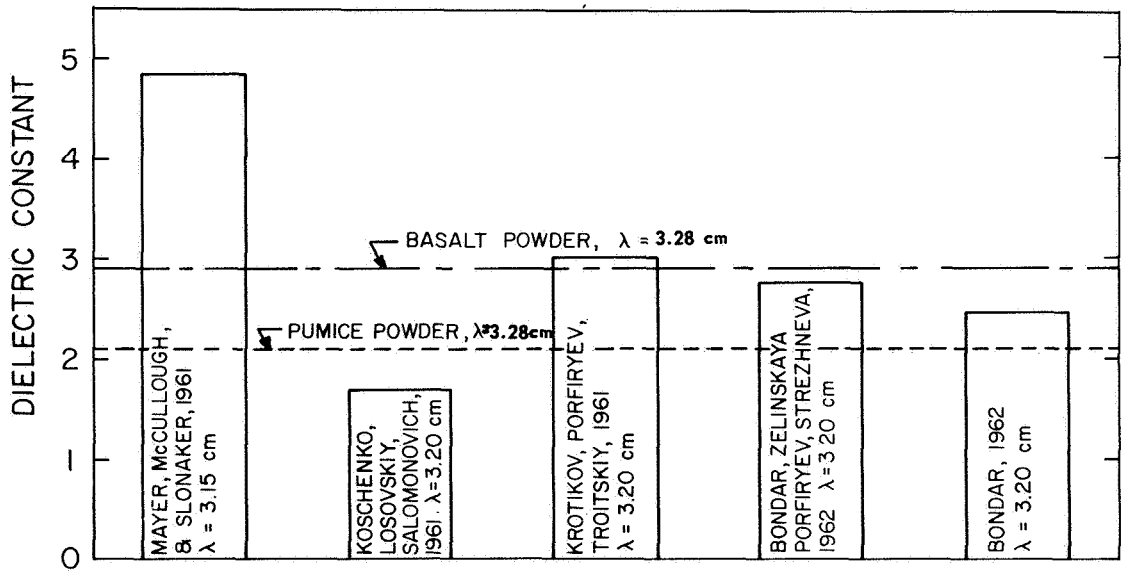

FIGURE 12. DIELECTRIC CONSTANT VALUES BASED ON INFRARED DATA, SET II

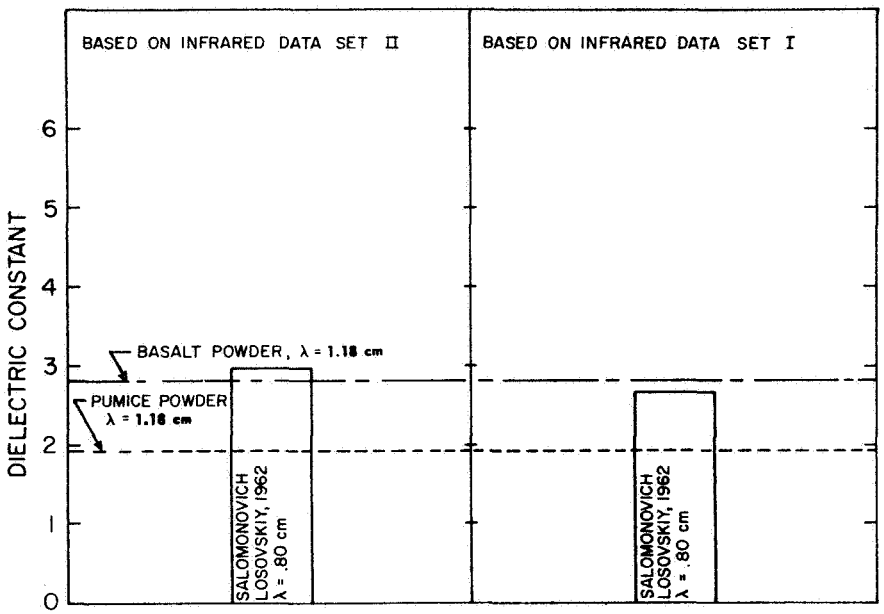

FIGURE 13. DIELECTRIC CONSTANT VALUES, $\lambda = 0.80$ cm

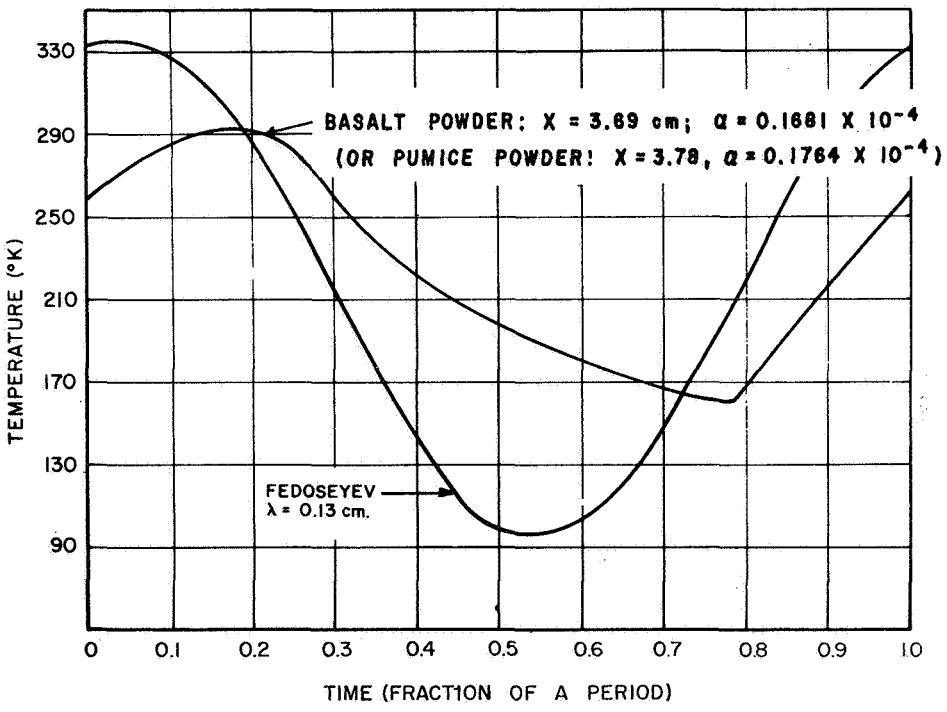

FIGURE 14. COMPARISON OF LUNAR MICROWAVE BRIGHTNESS TEMPERATURES WITH CALCULATED SUBSURFACE TEMPERATURES BASED ON INFRARED DATA, SET I (SINTON, LOW, AND SAARI)

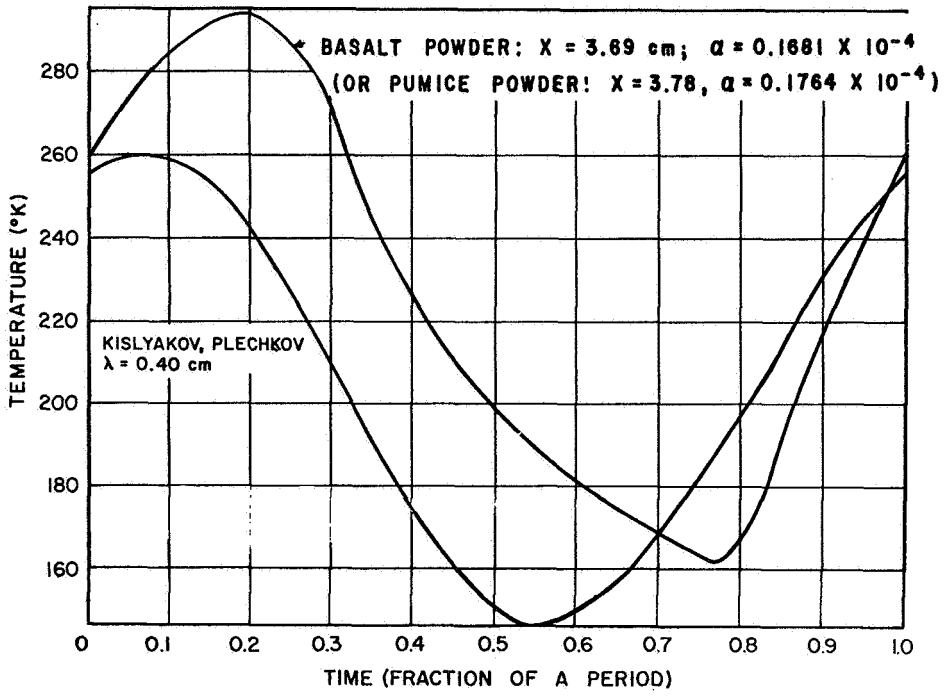

FIGURE 14. (Continued)

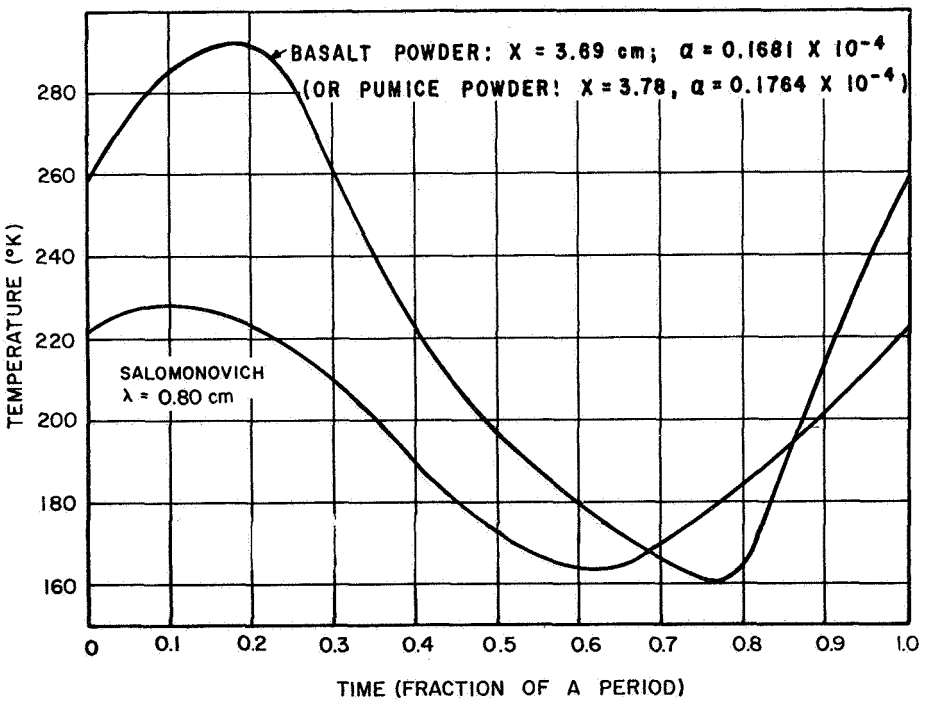

FIGURE 14. (Continued)

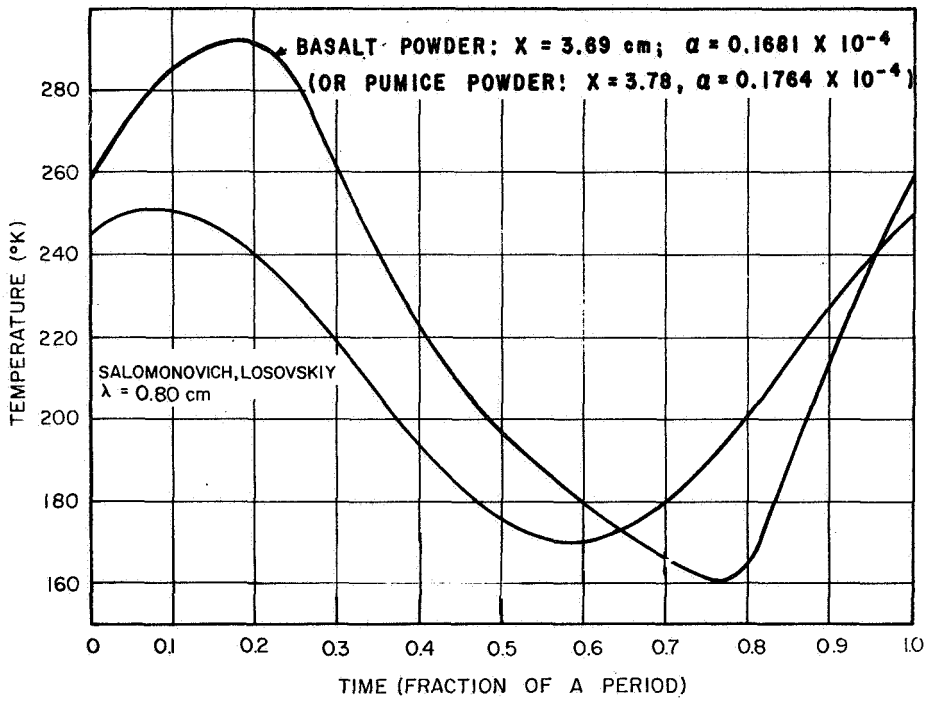

FIGURE 14. (Continued)

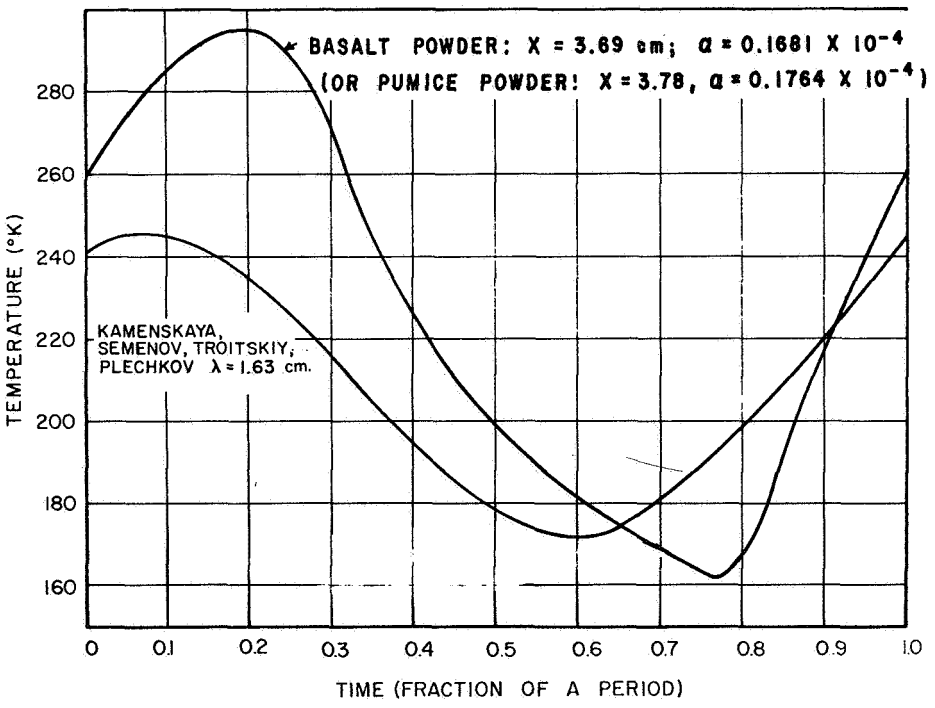

FIGURE 14. (Continued)

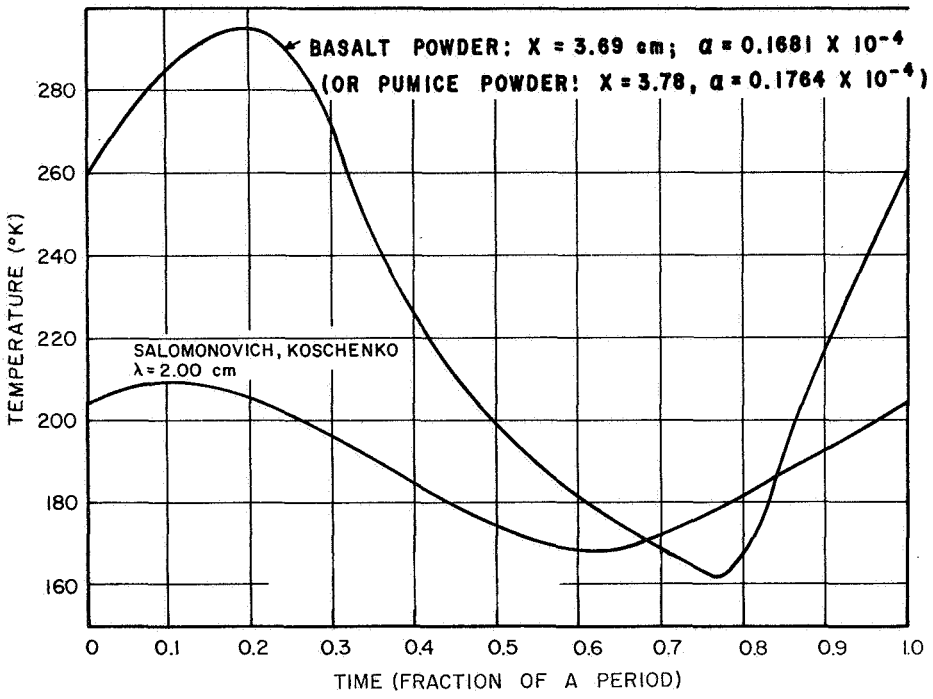

FIGURE 14. (Continued)

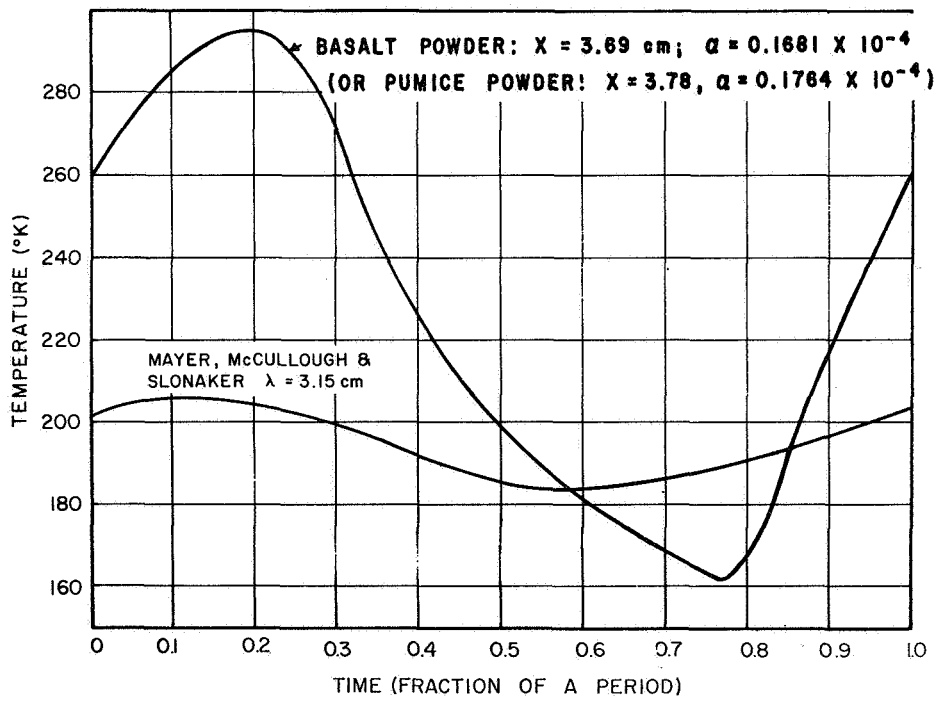

FIGURE 14. (Continued)

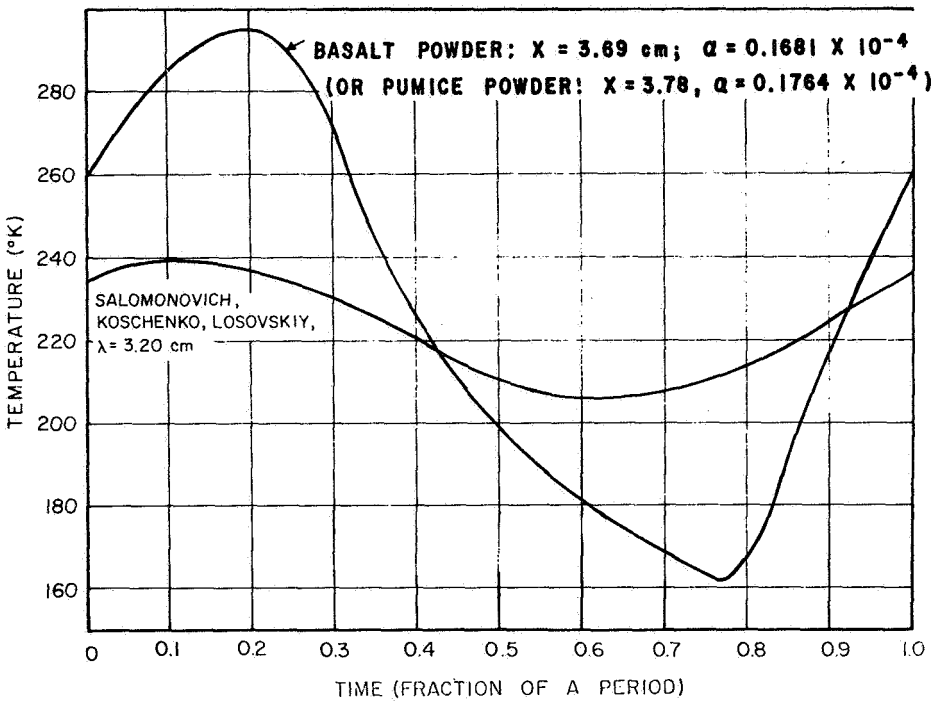

FIGURE 14. (Continued)

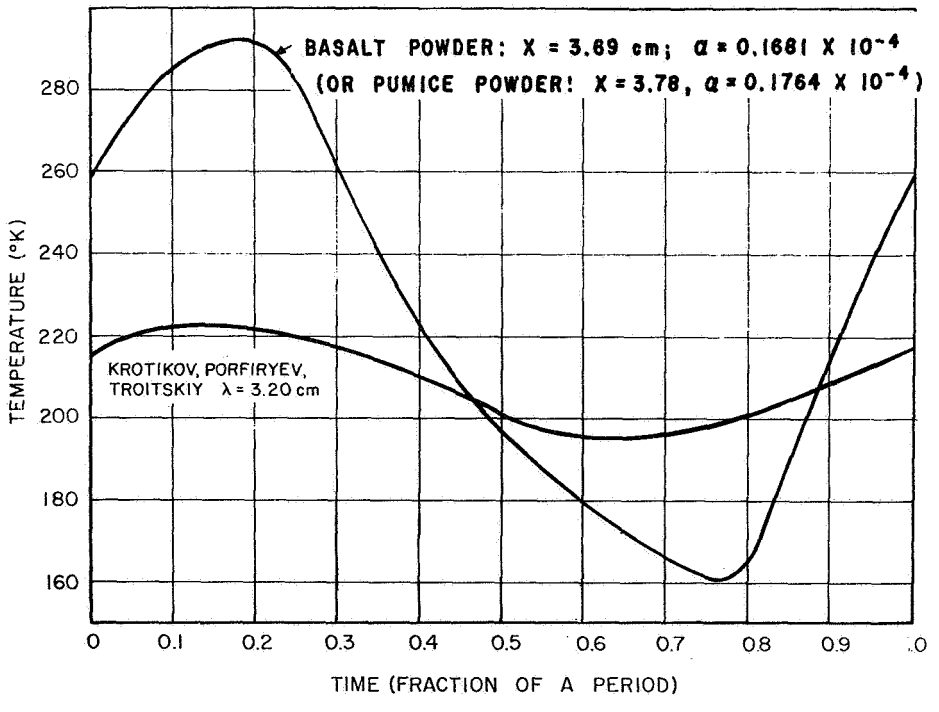

FIGURE 14. (Continued)

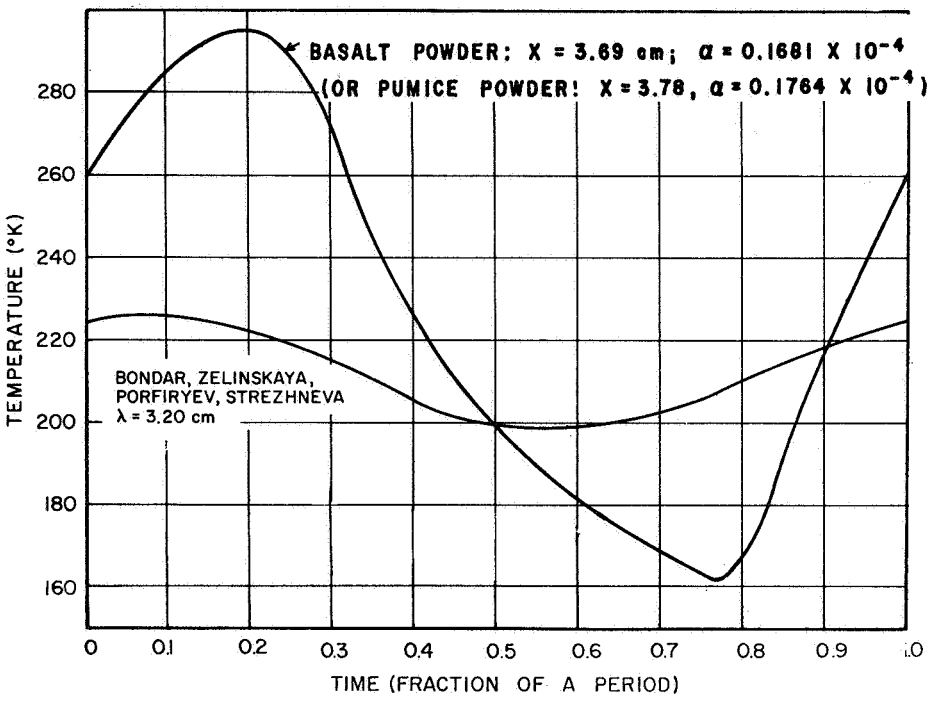

FIGURE 14. (Continued)

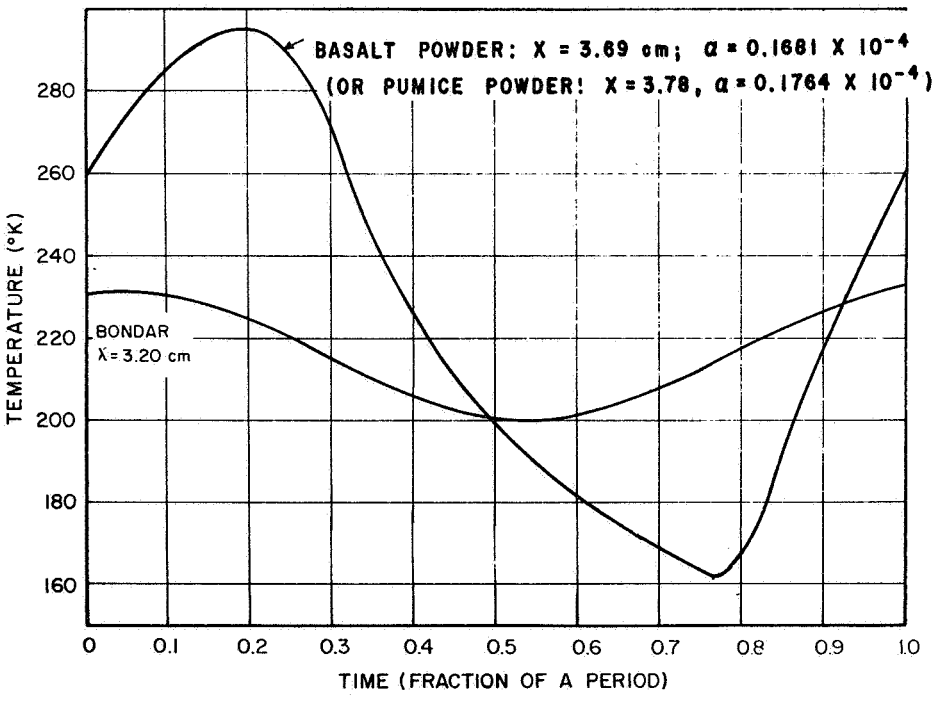

FIGURE 14. (Concluded)

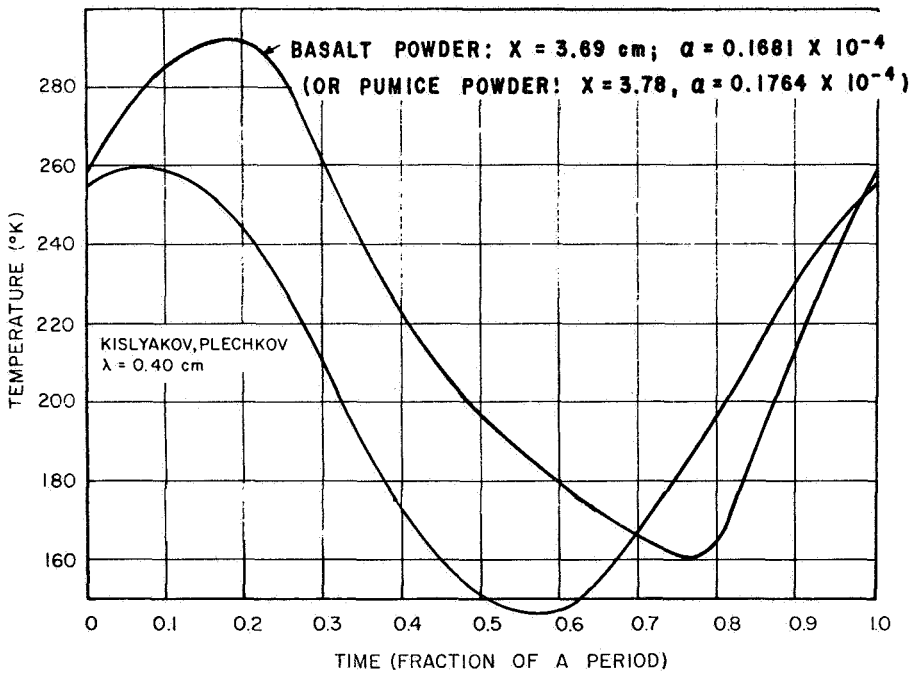

FIGURE 15. COMPARISON OF LUNAR MICROWAVE BRIGHTNESS TEMPERATURES WITH CALCULATED SUBSURFACE TEMPERATURES BASED ON INFRARED DATA, SET II (SINTON, LOW, MURRAY, AND WILDEY)

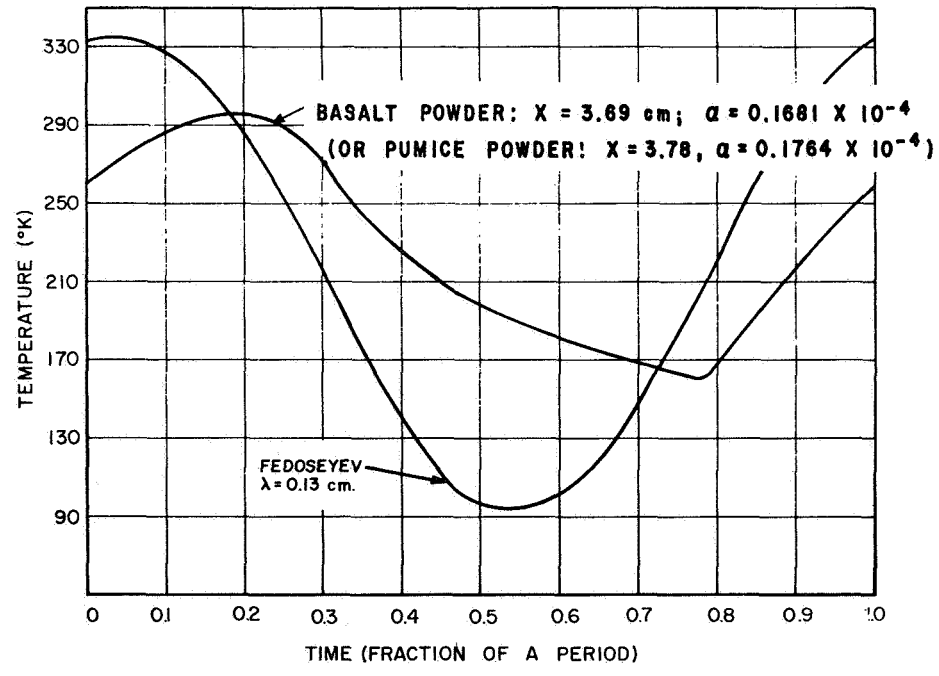

FIGURE 15. (Continued)

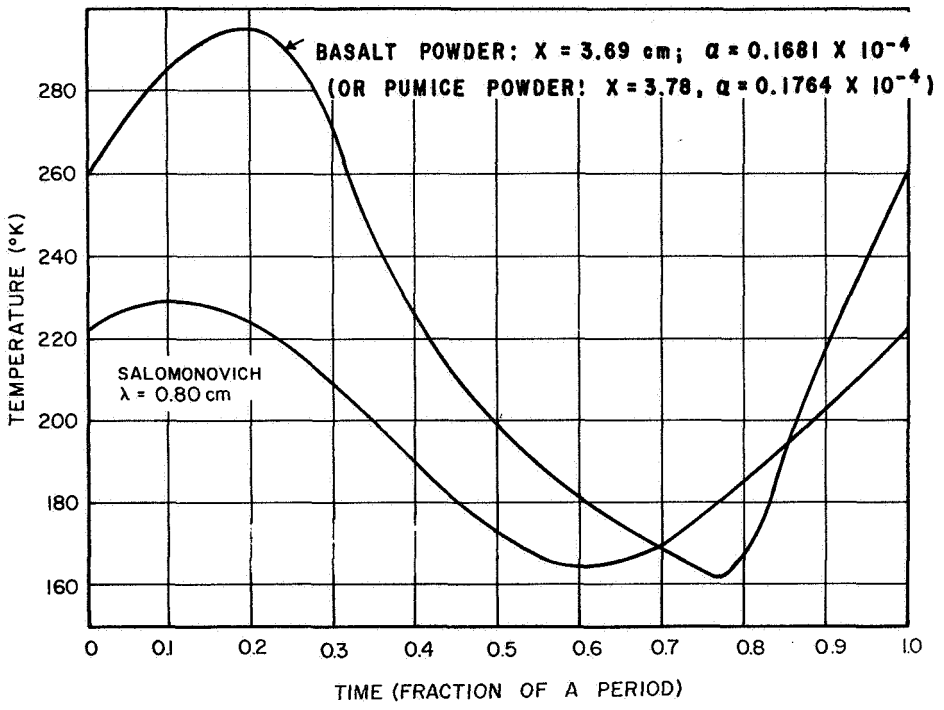

FIGURE 15. (Continued)

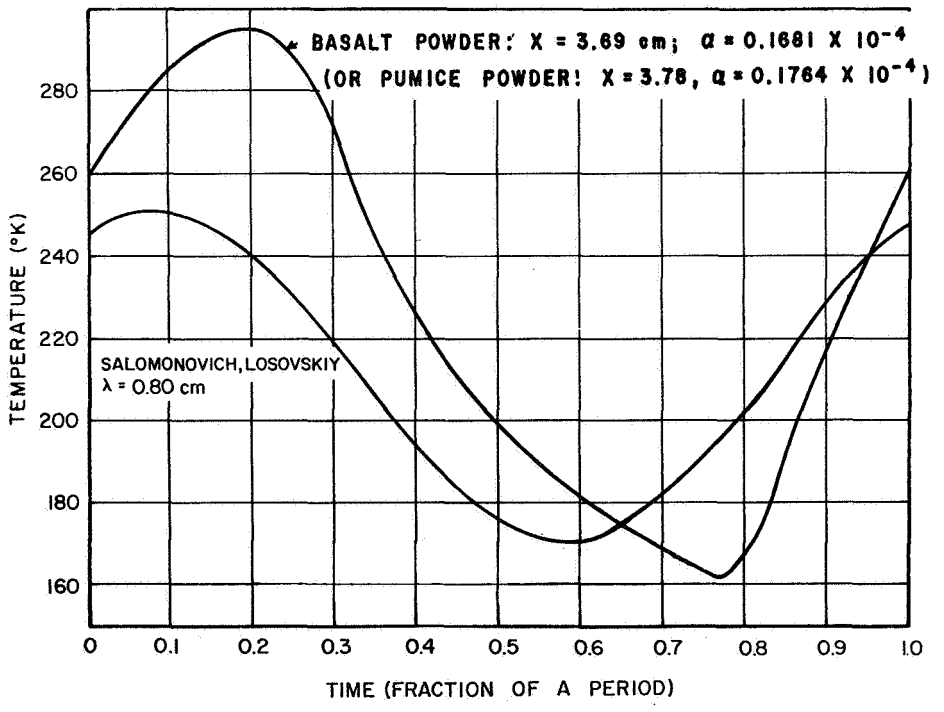

FIGURE 15. (Continued)

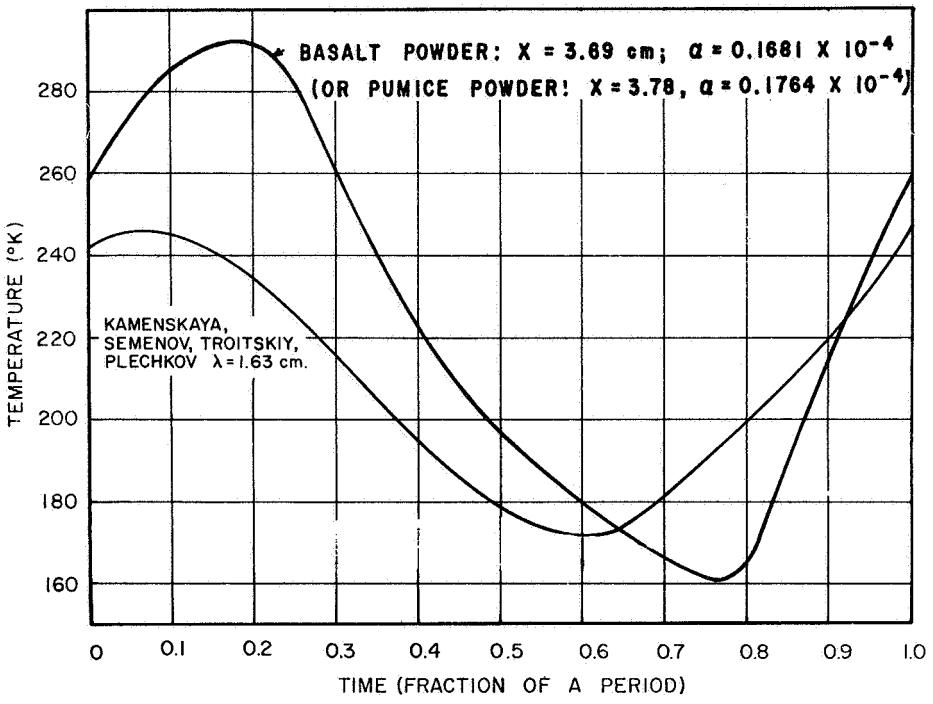

FIGURE 15. (Continued)

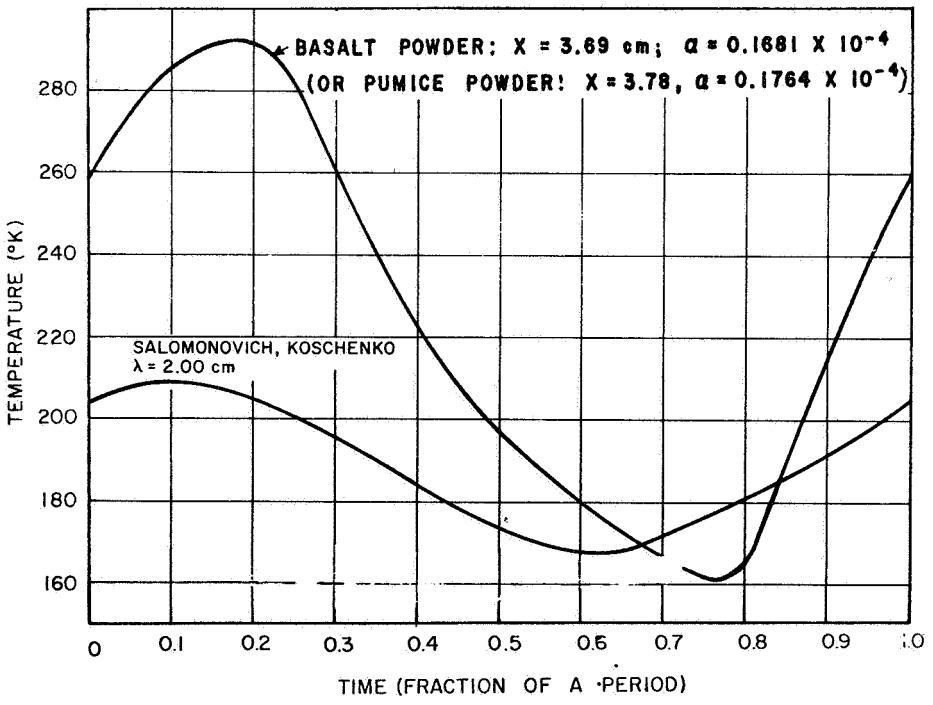

FIGURE 15. (Continued)

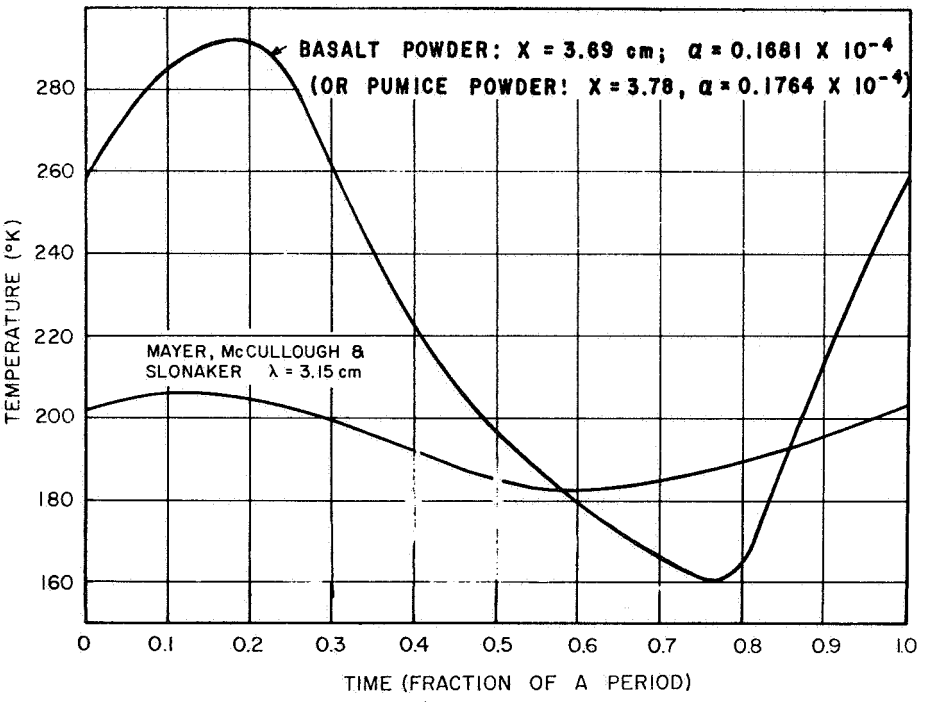

FIGURE 15. (Continued)

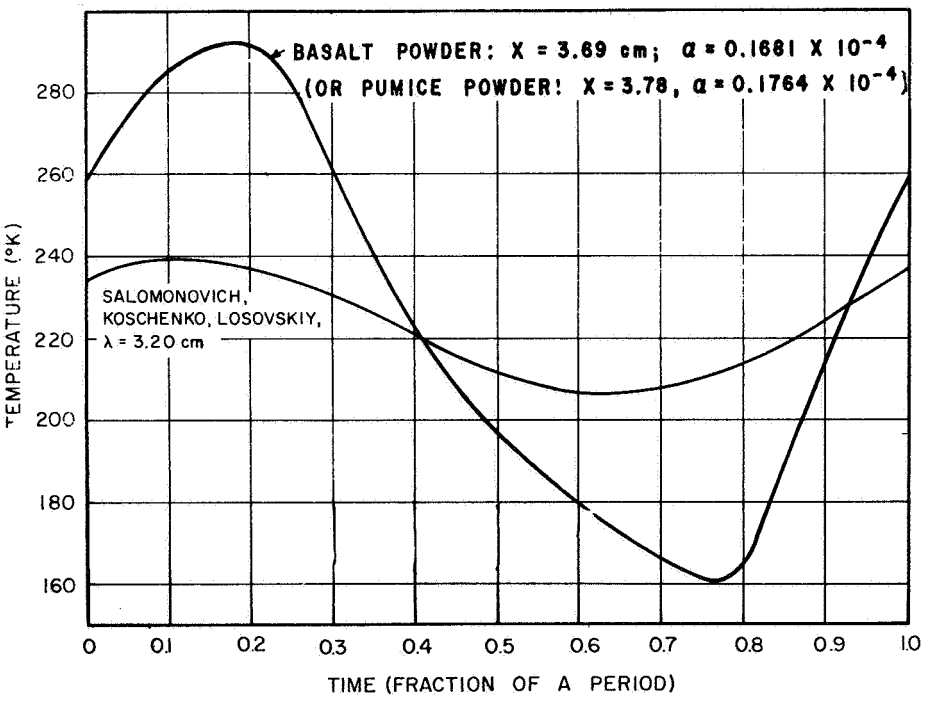

FIGURE 15. (Continued)

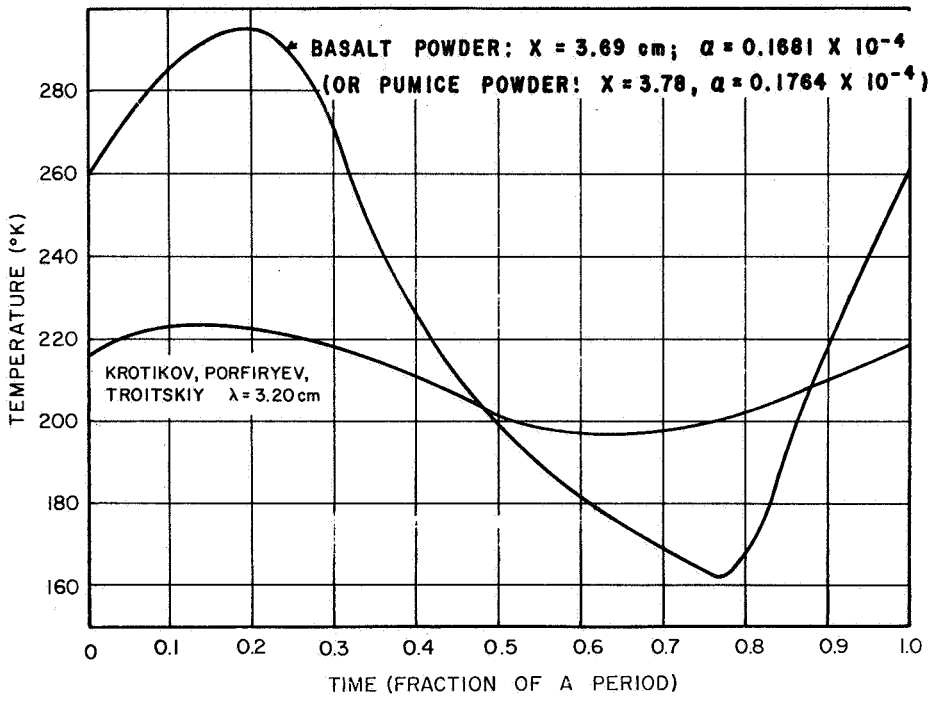

FIGURE 15. (Continued)

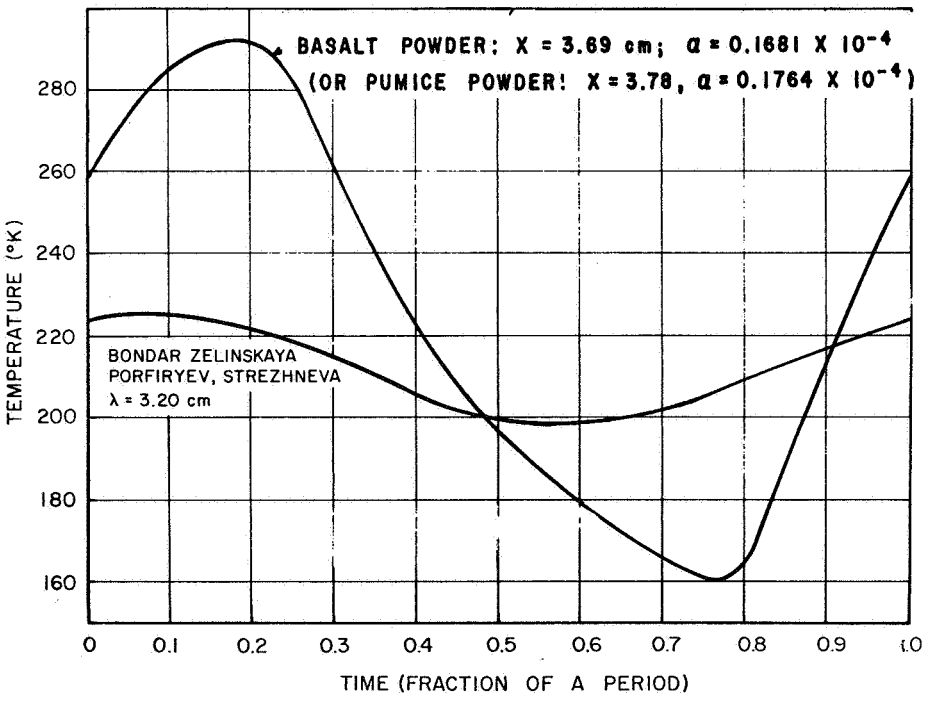

FIGURE 15. (Continued)

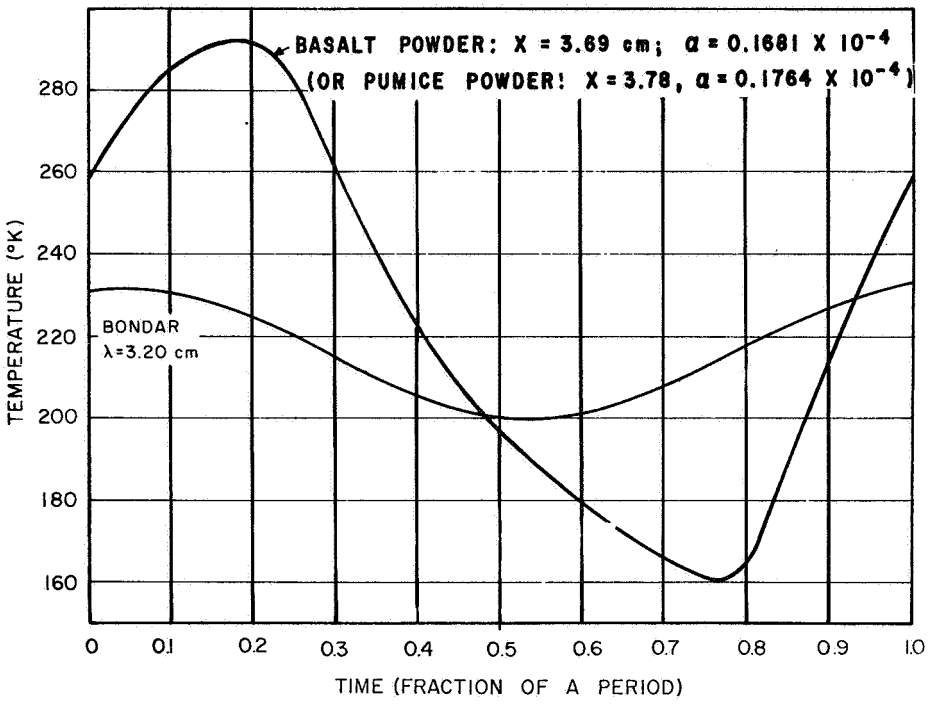

FIGURE 15. (Concluded)

REFERENCES

1. Ingersoll, L. R.; Zobel, O. J.; and Alfred C. Ingersoll: Heat Conduction with Engineering, Geological, and Other Applications. University of Wisconsin Press, Madison, 1959, pp. 78-81.

2. Hildebrand, F. B.: Introduction to Numerical Analysis. McGraw-Hill Book Company, Inc., New York, 1956, pp. 373-382.

3. Weaver, Harold: The Interpretation of Thermal Emission from the Moon. Solar System Radio Astronomy (Jules Aarons, Ed.), Plenum Press, New York, 1965, pp. 295-354.

4. Eggert, J. D.: Review of Lunar Microwave Emission. Interim Progress Report, RPL-24882-1, Contract No. NAS8-20166, January 10, 1967, Research Laboratories, Brown Engineering Company, Inc.

5. Krotikov, V. D.: Contribution to the Theory of Integral Radio Emission from the Moon. Soviet Radio Phys., vol. 6, no. 5, 1963, p. 889.

6. Hippel, Arthur von: Dielectrics and Waves. The M.I.T. Press, Massachusetts Institute of Technology, Cambridge, Mass., 1954, pp. 26-28.

7. Low, Frank J.: Lunar Nighttime Temperatures Measured at 20 Microns. Astrophys. J., vol. 142, no. 2, 1965, pp. 806-808.

8. Sinton, W. M.: Temperatures on the Lunar Surface. Chapter II (Z. Kopal, editor), Physics and Astronomy of the Moon, Academic Press, New York, 1962, p. 411.

9. Saari, J. M.: The Surface Temperature of the Antisolar Point of the Moon. ICARUS, vol. 3, July 1964, pp. 161-167.

10. Murray, B. C.; and Wildey, R. L.: Surface Nighttime Temperature Variations During the Lunar Nighttime. Contribution No. 1173 Division of Geological Sciences, CIT, Pasadena, California, May 17, 1963, p. 28.

11. Wechsler, A. E.; and Simon, I.: Thermal Conductivity and Dielectric Constant of Silicate materials. Final Report, Arthur D. Little Inc., NAS8-20076, December 1966.

NASA-Langley, 1969 —— 30 M426

NATIONAL AERONAUTICS AND SPACE ADMINISTRATION
WASHINGTON, D. C. 20546
OFFICIAL BUSINESS

FIRST CLASS MAIL

POSTAGE AND FEES PAID
NATIONAL AERONAUTICS AND
SPACE ADMINISTRATION

POSTMASTER: If Undeliverable (Section 158 Postal Manual) Do Not Return

"The aeronautical and space activities of the United States shall be conducted so as to contribute . . . to the expansion of human knowledge of phenomena in the atmosphere and space. The Administration shall provide for the widest practicable and appropriate dissemination of information concerning its activities and the results thereof."

—NATIONAL AERONAUTICS AND SPACE ACT OF 1958

NASA SCIENTIFIC AND TECHNICAL PUBLICATIONS

TECHNICAL REPORTS: Scientific and technical information considered important, complete, and a lasting contribution to existing knowledge.

TECHNICAL NOTES: Information less broad in scope but nevertheless of importance as a contribution to existing knowledge.

TECHNICAL MEMORANDUMS: Information receiving limited distribution because of preliminary data, security classification, or other reasons.

CONTRACTOR REPORTS: Scientific and technical information generated under a NASA contract or grant and considered an important contribution to existing knowledge.

TECHNICAL TRANSLATIONS: Information published in a foreign language considered to merit NASA distribution in English.

SPECIAL PUBLICATIONS: Information derived from or of value to NASA activities. Publications include conference proceedings, monographs, data compilations, handbooks, sourcebooks, and special bibliographies.

TECHNOLOGY UTILIZATION PUBLICATIONS: Information on technology used by NASA that may be of particular interest in commercial and other non-aerospace applications. Publications include Tech Briefs, Technology Utilization Reports and Notes, and Technology Surveys.

Details on the availability of these publications may be obtained from:

SCIENTIFIC AND TECHNICAL INFORMATION DIVISION

NATIONAL AERONAUTICS AND SPACE ADMINISTRATION

Washington, D.C. 20546